UNIVERSITÀ DEGLI STUDI DI MILANO

Scuola di Dottorato in Scienze Biologiche e Molecolari

XXIV Ciclo

BNip3: a potential target for the treatment of mitochondrial dysfunction in Huntington's disease.

Settore scientifico-disciplinare: BIO/06

Clarissa Colciago

Tutor: Dott.ssa Cappelletti, Dott.ssa Sassone, Prof.ssa Zippel

Coordinatore: Prof. Bolognesi

Anno Accademico 2010-2011

Contents

Part I

Abstract	pag. 3
State of the Art	pag. 4
Aim of the Project	pag. 8
Main Results	pag. 9
Conclusions and Future Prospects	pag. 39
References	pag. 42

Abstract

Huntington's disease (HD) is an autosomal dominant neurodegenerative disorder caused by the expansion of a CAG trinucleotide repeat in the *IT-15* gene. This disorder is characterized by progressive neuronal death in the basal ganglia and cortex. Although many years have passed since the discovery of the HD mutation, no therapy has shown a neuroprotective effect or has been shown to slow down the disease progression to date. Growing evidence supports a pivotal role for mitochondrial dysfunction in the death of patients' neurons but the molecular bases for mitochondrial impairment have not yet been elucidated. We provide the first evidence of an abnormal activation of Bcl-2/adenovirus E1B 19-kDa interacting protein 3 (BNip3) in cells expressing mutant huntingtin. In the present study we show abnormal accumulation and dimerization of BNip3 in mitochondria from human HD muscle cells and brain tissues from HD model mice. Recent results have suggested that cytotoxicity induced by mutant huntingtin is likely mediated by an alteration in normal mitochondrial dynamics, resulting in increased mitochondrial fragmentation. According to the literature, when BNip3 is overexpressed or induced, it localizes to the mitochondria and causes loss of mitochondrial potential, mitochondrial fragmentation and mitophagy. In this context, BNip3 could have a key role in mediating the impairment of mitochondrial dynamics in HD cells, and BNip3 blocking could improve mitochondrial function, representing a new therapeutic strategy for HD. We have characterized the effects of BNip3 blockade in cell culture model of HD by expression of the dominant negative protein BNip3ΔTM. BNip3ΔTM is a mutant protein deleted of the C-terminal domain that is necessary for BNip3 insertion into the outer mitochondrial membrane.

Importantly, we have demonstrated that blocking BNip3 expression and dimerization was able to restore normal mitochondrial phenotype in human HD muscle cells. Our data shed light on the molecular mechanisms underlying mitochondrial dysfunction in HD and point to BNip3 as a new potential target for neuroprotective therapy in HD.

State of the Art

Huntington's disease

Huntington's disease (HD) is a progressive neurodegenerative disorder characterized by motor disturbances, cognitive decline and behavioral changes. The disease has an autosomal dominant pattern of inheritance and an age-dependent penetrance. HD has a prevalence of 3-10 affected subjects per 100000 individuals in Western Europe and North America (Ho *et al*., 2001). Onset is most commonly in adulthood at about 40 years, with a typical duration of 15-20 years before premature death. The disorder was first described in the 19th century by George Huntington, but it was only the 1993 that the causative gene was finally isolated (The Huntington's Disease Collaborative Research Group, 1993). The disorder is caused by an expanded trinucleotide (CAG) repeat in the first exon of the *IT-15* gene, which is located on the short arm of chromosome 4 (4p16.3). The *IT-15* gene encodes a protein named huntingtin (htt) and the CAG expansion encodes an expanded polyQ stretch in the htt protein. Normal alleles contain 35 or less CAG repeats while mutant alleles are associated with 36 or more CAG repeats, although alleles with 36 to 39 repeats are considered to have reduced-penetrance.

The neurons of HD patients progressively die as the disease progresses, leading to widespread atrophy of the striatum and cortex, which account for the clinical symptoms of the disease. In the postmortem brains of patients with HD, extensive medium spiny neuronal loss was observed in the striatum and loss of pyramidal neurons was observed also in the cerebral cortex and hippocampus (Vonsattel and DiFiglia, 1998). The causes of selective and premature death of medium spiny projection neurons are not completely understood. Furthermore, HD is a multisystem disorder, wild-type (wt) and mutant htt (mhtt) proteins are expressed ubiquitously in the central and peripheral nervous systems of patients with HD. Htt is a large protein of unknown function without structural homology with any other known protein; however, deletion of the HD gene results in an early embryonic lethality (Duyao *et al*., 1995), revealing a role for the protein during the development. Within the cell wt htt is mainly localized in the cytoplasm associated with organelles (mitochondria, the Golgi apparatus, the endoplasmic reticulum, synaptic vesicles and several components of the cytoskeleton), but it is also present inside the nucleus, although to a lesser extent. Htt plays a role in protein trafficking, vesicle transport, postsynaptic signaling, transcriptional regulation, and apoptosis. The mutant protein has been shown to disrupt several of these intracellular pathways by abnormally interacting and/or sequestering key components of these multiple pathways, therefore the expanded polyglutamine is believed to confer a new function to htt that is toxic to the cell (toxic gain of function). On the other hand, several lines of evidence also suggest that a loss of function of wt htt also contributes to the disruption of intracellular homeostasis, culminating in neuronal dysfunction and death. Thus, a loss of function of the wt protein and a toxic gain of function of the mhtt contribute to the disruption of multiple

intracellular pathways. Various mechanisms of neurodegeneration such as mitochondrial dysfunction, oxidative stress, excitotoxicity, dopamine toxicity, metabolic impairment, apoptosis and autophagy have been implicated in HD. All these mechanisms are likely to occur in parallel and promote each other, ultimately culminating in neuronal loss.
Current therapies for HD provide control of some of the major troublesome signs and symptoms (chorea, psychosis, depression). However, these treatments are only "symptomatic", meaning that they ameliorate the clinical features of the illness, but the benefits are only temporary and disappear when the treatment is stopped. To date there are no drugs or agents available to treat or delay or prevent HD progression. Research's ultimate goal is to facilitate the development of therapeutic strategies for curing the disease or, as an alternative, for slowing or stopping its progression.

Mitochondrial defects in HD

Growing evidence suggests that mitochondrial dysfunction has a key role in HD pathogenesis (Browne, 2008). In particular, observations that mitochondrial changes detected in HD genetic models are very early events that precede disease onset support the hypothesis that mitochondrial impairment may occur early enough to contribute to the underlying pathogenetic mechanisms. Several studies suggest that abnormal mitochondrial bioenergetics is involved in HD pathogenesis. Studies in HD patients have shown a significant decrease in glucose uptake in the cortex and striatum (Kuhl *et al*., 1982). Magnetic resonance imaging spectroscopy (MRI) showed increased production of lactate in cerebral cortex and basal ganglia from HD patients (Jenkins *et al*., 1993; Koroshetz *et al*., 1997). Studies using MRI of postmortem brains from HD patients revealed a progressive atrophy of the striatum, compared to brain images of age-matched control subjects (Bamford *et al*., 1989). Biochemical studies of brain tissue from HD patients have demonstrated multiple defects in the caudate, as a reduced activity of several components of oxidative phosphorylation (Stahl and Swanson, 1974; Butterworth *et al*., 1985). Striatal cells derived from a knock-in mouse model of HD show significantly diminished oxidative phosphorylation indicated by lower respiration and mitochondrial ATP production rates compared to wild-type cells (Milakovic and Johnson, 2005). Also ultrastructural abnormalities in mitochondria have been described in HD cortical tissue (Gardian and Vecsei, 2004). Studies on peripheral tissues and peripheral cells (fibroblasts, lymphoblasts and myoblasts) from HD patients have identified several mitochondrial abnormalities, including a decreased activity of respiratory chain enzymatic complexes, a decreased ATP/ADP ratio and an altered morphology of these organelles (Squitieri *et al*., 2010; Costa *et al*., 2010). Overall, findings from these studies suggest that defective mitochondrial bioenergetics plays a large role in the progression and pathogenesis of HD.

Mitochondria have an essential role in the physiology of eukaryotic cells; not only do they produce most of the cell's ATP but they also participate in ion homeostasis, regulation of the cell's redox state, lipid and amino-acid metabolism, as well as in regulation of programmed cell death. All these functions are highly dependent on the mitochondrial electrochemical transmembrane potential ($\Delta\psi_m$), a physicochemical parameter consisting of two components, namely the total transmembrane electrical potential (voltage gradient) and the proton gradient that is physiologically generated across the inner mitochondrial membrane by the activity of the respiratory chain. Growing evidence indicates that the many mitochondrial abnormalities observed in HD tissues may stem from an abnormal $\Delta\psi_m$, as the mitochondria extracted from HD patients had $\Delta\psi_m$ values lower than the mitochondria from normal patients (Sawa *et al*., 1999; Panov *et al.,* 2002; Ciammola *et al*., 2006; Almeida *et al*., 2008). $\Delta\psi_m$ loss seems to be a direct effect of mhtt, given that it occurs in normal cells transfected with mhtt (Bae *et al*., 2005; Benchoua *et al.,* 2006), and when mhtt is added to mitochondria isolated from normal brains (Panov *et al*., 2003). The results from these studies notwithstanding, the molecular bases for the $\Delta\psi_m$ decrease observed in HD cells still remain elusive. Depolarization of mitochondria is known to induce their fragmentation into multiple smaller organelles (Legros *et al*., 2002) by inhibiting organelle fusion. Furthermore recent studies uncovered an interplay between HD and mitochondrial dynamics. Once thought to be static in their organization, mitochondria are now considered to constitute a population of organelles that migrate throughout the cell, fuse and divide (fusion and fission mechanisms), and undergo regulated turnover. Studies performed over the past decade, revealed that mitochondria form a wide network of long tubules called mitochondrial network and that mitochondrial energy production is controlled by elongation or fragmentation of the tubular network organization. They also revealed that disruption of mitochondrial dynamics and bioenergetic defects are closely linked showing that the pathological contexts determine modifications of the mitochondrial–network that in turn controls bioenergetics (Benard and Rossignol, 2008). In particular, several observations indicate that mitochondria undergo rapid, extensive fragmentation early in several cell death pathway thus suggesting a relationship between mitochondrial dynamics and apoptotic conditions (Knott *et al*., 2008). In healthy neurons, fission and fusion mechanisms balance equally to maintain tubular mitochondrial shape. But there is important evidence to suggest that in HD the balance between mitochondrial fission and fusion is abnormal and that HD cells are characterized by mitochondrial fragmentation. HeLa cells overexpressing a mhtt with a 74 glutamine repeats show fragmentation of mitochondria, reduced mitochondrial fusion, reduced ATP and increased cell death (Wang *et al*., 2009). Remarkably, expression of either dominant–negative Drp1 (a protein that induce mitochondrial fission) or Mfn2 (protein that induce mitochondrial fusion) not only prevents this change in mitochondrial morphology, but also restores ATP levels and attenuates cell death. Moreover, according to a recent report, various cellular models of HD (including immortalized striatal cell lines isolated from knock–in HdhQ111 mouse, primary striatal neurons from YAC128

mice and lymphoblasts from HD patients) are characterized by mitochondrial fragmentation and cristae alterations (Costa *et al*., 2010). Overall these data suggest that mhtt causes an impairment of mitochondrial dynamics.

BNip3

Bcl-2/adenovirus E1B 19-kDa interacting protein 3 (BNip3) is a member of the so-called BH3-only subfamily of Bcl-2 family proteins that regulate the permeability state of the outer mitochondrial membrane (OMM). This regulation is accompanied by the formation of homo- and hetero-oligomers inside the membrane, which influences $\Delta\psi_m$ and controls cell death mechanisms (Harris *et al*., 2000; Frazier *et al*., 2006). The BNip3 protein is normally present in the brain tissue and skeletal muscle (Lee *et al*., 2006) and is mainly localized in the cytoplasm and nucleus or is found loosely associated with the mitochondrial membrane in an inactive conformation (Burton *et al*., 2006; Webster *et al*., 2005). The molecular mechanism underlying BNip3 activation is not completely understood, but it probably involves a multi- step process. A few intracellular toxic stimuli, such as decreased intracellular pH and increased cytosolic calcium concentration (Webster *et al*., 2005; Graham *et al*., 2007), can induce BNip3 integration into the OMM with the protein's N terminus in the cytoplasm and C terminus inside the mitochondria (Vande Velde et al., 2000). The BNip3 C-terminal hydrophobic domain is required for integration in the OMM, as its deletion prevents the mutant protein (BNip3ΔTM) from integrating into the OMM and inducing cell death (Ray *et al*., 2000; Kim *et al*., 2002). Once integrated into the OMM, BNip3 can self-associate and form stable homodimers on the basis of intermonomeric helix–helix polar interactions of various side chains (Bocharov *et al*., 2007). The unique structure of the transmembrane domain suggests that BNip3 dimers could function as proton channels in the OMM, thereby increasing ion conductance (Bocharov *et al*., 2007). BNip3 integrates into the OMM through its C terminal transmembrane domain (TM) leaving the last 10 residues into the intermembrane space (Vande Velde *et al*., 2000), where it can interacts with the pro-fusion protein OPA1 altering the mitochondrial dynamics (Landes *et al*., 2010). Several studies have previously reported that BNip3 can cause changes in mitochondrial morphology in cell lines. A lot of evidence shows that activated BNip3 induces mitochondrial fragmentation and mitophagy. In fact the examination of mitochondria in BNip3-overexpressing cardiac myocytes reveals extensive fragmentation of the mitochondrial network (Hamacher Brady *et al*., 2007). Moreover, overexpression of HA-BNip3 in HeLa cells results in fragmentation of mitochondria and this fragmentation depends on Drp1 activity (Landes *et al*., 2010). The dominant-negative mutant BNip3ΔTM is able to interact with wild-type BNip3 and block its integration into the OMM (Hamacher-Brady *et al*., 2007; Kubasiak *et al*., 2002; Regula *et al*., 2002). The overexpression of BNip3ΔTM results in normal filamentous mitochondrial network (Hamacher-Brady *et al*., 2007).

Aim of the Project

The importance of mitochondria in HD pathogenesis has long been investigated, but research on how mhtt affects the mitochondrial functions and dynamics (fission and fusion, fragmentation and mitophagy) is still lacking. To date there are no reported studies about the role of BNip3 protein as mediator of mitochondrial functions and dynamics in HD. Considering the crucial role of BNip3 in regulating OMM permeability and of mitochondrial dynamics, we have undertaken a study to investigate the potential role of BNip3 in the mitochondrial dysfunction induced by mhtt.

The first aim of the current study was to investigate the role of BNip3 in mhtt expressing cells and mouse model of HD. To address the role of BNip3 in HD we examined its activation and mitochondrial localization. This study was carried out using cell and mouse models of HD. Data regarding BNip3 activation and localization were investigated in brain tissues from R6/2 and YAC mice (mouse models of HD) and in primary cells obtained from muscular biopsies from HD patients.

The second aim of the current study was to characterize the downstream effects of BNip3 activation on mitochondria in HD. We performed these analyses in HD neuronal cell models (mouse striatal cell line) and in primary cells obtained from muscular biopsies from HD patients. In vitro HD cell cultures were analyzed for mitochondrial morphology and parameters (including mitochondrial potential, mitochondrial mass, ATP synthesis and oxygen consumption).

The third aim of the current study was to investigate therapeutic strategies connected to BNip3 inactivation in cell models. We analyzed whether BNip3 can be considered a therapeutic target to improve mitochondrial function in HD. Therefore we addressed what would happen in mhtt expressing cells when transfected with BNip3ΔTM. We transiently expressed BNip3ΔTM in HD neuronal cell models and HD myoblast cells in order to verify if the expression of the dominant negative form of BNip3 was able to restore the normal mitochondrial phenotype.

Main Results

Increased BNip3 levels and mitochondrial localization in muscle cells from HD patients.

To investigate the potential role of BNip3, we analyzed its expression levels in muscle cell lysates from four HD and four control subjects by SDS-PAGE. According to the literature peripheral cells of HD patients display mitochondrial abnormalities related to mhtt expression (Sassone *et al*., 2009). In particular, HD muscular cells are a useful cell culture model that mirrors many mhtt related dysfunctions that have been shown in neuronal cells (Ciammola *et al*., 2006; Ciammola *et al*., 2010).

The molecular weight of BNip3, as predicted from its amino-acid sequence, is 21.5 kDa; however, the protein has been described to migrate as two major molecular species, with apparent molecular weights of ~30 and ~60 kDa in SDS-PAGE gels, representing monomeric and dimeric forms, respectively (Chen *et al*., 1997; Mellor and Harris, 2007). The apparent molecular weight of monomeric BNip3 in SDS-PAGE and the presence of multiple protein bands at ~30 kDa are likely due to protein phosphorylation, as BNip3, similar to many proteins of the Bcl-2 family, bears consensus sites for phosphorylation by protein kinases (Graham *et al*., 2007).The biological role of these possible posttranslational modifications still remains unknown. The BNip3 signal at ~60 kDa, corresponding to BNip3 dimers, can be detected by SDS-PAGE, as BNip3 dimers are highly stable and resistant to detergents (Chen *et al*., 1997; Tracy and Macleod, 2007). In cell lysates from human HD myoblasts, we detected monomeric BNip3. Densitometric analysis showed higher levels of monomeric BNip3 in HD myoblasts than in myoblasts extracted from control subjects. Dimeric BNip3 was barely detectable in total lysates of human myoblasts (Fig. 1a). As the pivotal step in BNip3-mediated cell death involves its integration into the OMM (Vande Velde *et al*., 2000), we tested whether the increased expression of BNip3 resulted in increased mitochondrial localization. Mitochondria-enriched fractions were prepared from normal and HD human muscle cells and then treated by alkaline pH. This treatment detaches loosely associated peripheral membrane proteins (Goping *et al*., 1998), thus enriching the samples for mitochondrial transmembrane proteins. Immunoblot analysis of alkali-treated mitochondrial fractions showed strong monomeric BNip3 signals in both HD and control myoblasts. However, there was a trend of increased monomeric BNip3 in HD samples. The dimeric form of BNip3 was visible only in the HD mitochondria and was not detectable in control myoblasts (Fig. 1b). HD myoblasts derived from patients carrying 60 CAG repeats (lane 6) had the highest dimeric BNip3 signal. To confirm the increased association of BNip3 with the HD mitochondria, we performed confocal microscopy on myoblasts obtained from control and HD patients. Notably, BNip3 colocalized with the mitochondria in ~40% of HD cells, while the protein was mainly localized in the cytoplasm and in the nucleus in

control cells (Fig. 1c). Overall, our data suggest the accumulation and dimerization of BNip3 protein in the mitochondria of human HD muscle cells.

BNip3 levels in the brain tissue from R6/2 and YAC128 mouse models.

To investigate whether the changes observed in BNip3 expression and localization in muscle cells obtained from HD patients mirrored events occurring in the CNS, we analyzed BNip3 levels and localization patterns in the brain tissues of two different HD model mice, namely R6/2 and yeast artificial chromosome (YAC)128. R6/2 mice are transgenic for exon-1 of the human *IT-15* gene, containing highly expanded CAG repeats (Mangiarini *et al*., 1996), whereas YAC128 mice express a full-length *IT15* gene with 128 CAG repeats (Hodgson *et al*., 1999). There was a trend of decreased monomeric BNip3 in HD striatum samples (Fig. 2a); no significant difference in BNip3 expression was observed in the cortex from R6/2 and littermate control mice at 10 weeks of age (Figure 2b). It is noteworthy that immunoblotting analysis of alkali-treated mitochondrial fractions showed a stronger dimeric BNip3 signal in the R6/2 striatum than in the wild-type striatum (Fig. 2c). In R6/2 mitochondrial fractions, we also observed an anti-BNip3-immunoreactive band with an apparent molecular weight >60 kDa, which is consistent with previously described higher-order oligomeric forms of BNip3 (Frazier *et al*., 2006; Gao *et al*., 2005). Immunoblotting analysis of cortical mitochondrial fractions showed a slight increase in the dimeric BNip3 signal in the R6/2 striatum than in the wild-type striatum, but the difference did not reach statistical significance (Fig. 2d). In the striatum of 6-month-old YAC128 mice, levels of monomeric and dimeric BNip3 were significantly increased with respect to control littermates (Fig. 2e). Expression levels in the cortex showed a high degree of variability among the animals analyzed, and mean differences between control and HD mice did not reach statistical significance (Fig. 2f). However, the variance in the distribution of BNip3 levels in the HD group was significantly different from the variance in the control group of animals, suggesting a trend toward increased BNip3 levels in HD cortexes. Similar to R6/2 animals, the mitochondria from the YAC128 striatum contained more BNip3 than those from the control striatum (Fig. 2g). No difference in BNip3 level was detected between the YAC128 cortical mitochondria and the mitochondria from control cortexes (Fig. 2h).

***Increased resistance of monomeric BNip3 in HD samples to proteinase-K digestion*.**

One proposed model to explain BNip3 function posits that BNip3 can exist as an inactive, latent monomer, which requires a death activation signal to become active (Tracy and Macleod, 2007).

The death signal elicits a conformational change in monomeric BNip3 that promotes protein dimerization or oligomerization in the lipid environment of the mitochondrial membrane and the formation of an ion-permeable channel through the OMM. Thus, a conformational change in the monomeric form is believed to be the triggering event in BNip3 activation and mitochondrial membrane permeabilization. To assess potential differences in the conformational state of monomeric BNip3 induced by mutant htt, we tested BNip3 resistance to in vitro digestion with proteinase-K (PK) in whole extracts of HD samples. This approach has been successfully used to discriminate between inactive (more prone to digestion) and active (more resistant) forms of monomeric BNip3 in a previous study (Frazier *et al*., 2006). The increased resistance of the active monomeric form to PK digestion is presumably due to the acquisition of a proteolysis-resistant conformation (Frazier *et al*., 2006). Total lysates prepared from control and HD myoblasts were digested with increasing concentrations of PK, and the products were analyzed by immunoblotting. As shown in Fig. 3a, BNip3 monomers in cell lysates from HD myoblasts were significantly more resistant to PK digestion than those from control samples. Actin digestion was not different between HD and control samples (Fig. 3a), demonstrating that the increased resistance to proteolysis in HD samples was specific for the BNip3 protein. Similar results were obtained using total protein extracts from R6/2 and control mouse brains (Fig. 3b). Overall, our data support the hypothesis that mutant htt promotes a conformational change in the BNip3 protein that may trigger its activation.

To further confirm that BNip3 activation in HD sample involve a post-trascriptional mechanism, we evaluated BNip3 mRNA expression by real-time PCR experiments. We firstly examined the expression pattern of BNip3 in HD and control myoblasts. Results showed a slight increase in BNip3 mRNA in HD myoblasts compared with control myoblasts (Fig.4a). No difference in BNip3 mRNA was detected in R6/2 brains compared with brains of littermate controls, and in YAC128 brains compared with wild-type brains (Fig. 4b-c).

Decreased JC–1 ratio in HD cells.

JC–1 is a mitochondrial dye that stains mitochondria in living cells in a membrane potential–dependent fashion, but JC–1 fluorescence is dependent also on the mitochondrial mass content. JC–1 ratio is widely used to measure the $\Delta\psi_m$. Ciammola *et al*. previously reported that HD myoblasts have $\Delta\psi_m$ value that is decreased by ~30% compared with control myoblasts (Ciammola *et al.,* 2006). We have analyzed mitochondrial $\Delta\psi_m$ in a mouse cell model of HD. Striatal cell lines have been established by Trettel and colleagues from HD knock in (HdhQ111/Q111) and wild–type (HdhQ7/Q7) mice (Trettel *et al*., 2000). The STHdhQ111/Q111 cell line expresses mhtt at endogenous levels, and therefore it is a genetically accurate cell model

of HD. As the striatum is the most affected region in HD, the striatal origin of this cell model makes it optimal for HD studies.
We measured JC−1 ratio in STHdh cells maintained in mild metabolic stress condition for three days, by using a medium that forces cells to depend on mitochondrial respiration for energy production (DMEM without D−glucose supplemented with 10% fetal bovine serum, 5mM galactose, 5 mM sodium pyruvate; see references Robinson *et al*., 1992, Palmfeldt *et al*., 2009). We observed that $\Delta\psi_m$ was decreased by ~ 70% in STHdhQ111/Q111 cells compared to STHdhQ7/Q7 (Fig. 5; **p< 0.01).

Decreased mitochondrial mass content in HD cells.

We further examined mitochondrial mass in STHdhQ7/Q7 and STHdhQ111/Q111 cells (maintained in mild metabolic stress condition for three days as described in the previous paragraph) loading the cells with the mitochondria specific dye MitoTracker Green FM (Agnello *et al.,* 2008). MitoTracker is a fluorescent dye that localizes to the mitochondrial matrix regardless of the mitochondrial membrane potential and covalently binds to mitochondrial proteins by reacting with free thiol groups of cysteine residues.
Fluorescent cells were then analyzed with a FACScan flow cytometer. The data confirmed that STHdhQ111/Q111 cells had a reduced mitochondrial mass compared to control cells (Fig. 6a).
To test whether lower mitochondrial content is associated with the expression of mhtt in human myoblasts we measured mitochondrial DNA copy number by real time PCR in 8 control myoblasts and 6 HD myoblasts. Relative mitochondrial DNA copy number was quantified by the ratio of mitochondrial gene (mitochondrial D-loop) to a nuclear gene (RNaseP) and the mean mtDNA content (expressed as the relative number of mtDNA copies per nuclear genome) was 4646 in the control myoblasts and 4107 in HD myoblasts (Fig.6b). Results indicate that HD muscle cell cultures display a trend in reduction of mitochondrial DNA copy number as compared to control myoblasts, which is consistent with results obtained in STHdh cells and with literature. We need to replicate this experiment in a larger cohort of muscle cells.

Increased mitochondrial fragmentation in cells expressing mhtt

To better understand the possible involvement of BNip3 activation in the mitochondrial alteration induced by mhtt, we examined mitochondrial morphology in STHdh cells. STHdhQ7/Q7 and STHdhQ111/Q111 cells were transiently transfected with plasmid encoding mitochondrially targeted fluorescent protein (pDsRed2−Mito) and 400 randomly chosen cells per group were

analyzed by fluorescence microscopy. Cells were analyzed by two different blinded observers and scored as containing predominantly fragmented or predominantly elongated mitochondria according to a described protocol (Chen *et al.*, 2005). No differences were observed between STHdhQ7/Q7 and STHdhQ111/Q111 cells maintained in normal growth conditions (DMEM supplemented with 10% fetal bovine serum) but when cell cultures were exposed to mild metabolic stress for three days, STHdhQ111/Q111 cells exhibited an increased mitochondrial fragmentation as compared to STHdhQ7/Q7. Figure 7a is representative of the analyzed images. As shown in figure 7b, about 81% of STHdhQ111/Q111 cells after three days in galactose medium displayed fragmented mitochondria and only 19% contained elongated mitochondria, whereas 40% of STHdhQ7/Q7 had elongated mitochondria (Fig. 7b; chi–square test, $p<0.01$). When cell cultures were exposed to mild metabolic stress for six days we have obtained similar results (Fig. 7c; chi-square test, $p<0.05$). To better describe the morphometry of the mitochondrial network, we analyzed the confocal fluorescence images for an automated shape–analysis of the mitochondrial structures. By means of ImageJ 1.42, raw images were binarized, mitochondrion number (nc), area and outline were measured and the form factor was calculated (defined as $[P_m^2]/[4\pi A_m]$), where P_m is the length of the mitochondrial outline and A_m is the area of the mitochondrion. The form factor allows quantifying the degree of branching of the mitochondrial network. Images of twelve randomly selected cells per genotype were analyzed (Koopman WJ et al., 2006). FF was lower in STHdhQ111/Q111 compared to STHdhQ7/Q7, this data confirms a decrease of mitochondrial length and branching in HD cells (Fig. 7d represents mean ± SEM; *$p<0.05$ vs STHdhQ7/7). The analysis also revealed that STHdhQ111/Q111 cells had a lower number of mitochondria per cell (Fig. 7e represents mean ± SEM; *$p<0.05$ vs STHdhQ7/7).

We next analyzed mitochondrial morphology in *in vitro* muscular cells obtained from muscular biopsy of HD patients. Myoblasts from 3 HD patients (CAG repeat on the upper allele were 59, 50 and 50) and 3 healthy controls were transfected with pDsRed2–Mito and a comparative analysis of mitochondrial morphology was performed. Figure 8a is representative of the analyzed images. For each subject 300 cells were randomly chosen and scored into three categories. Class I cells: complete fragmentation resulting in only mitochondrial spheres; Class II cells: extensive fragmentation but contained some very short mitochondrial rods (<5 μm in length); Class III cells: cells with medium–length mitochondrial tubules (>8 μm in length). The analysis in three categories was possible as myoblasts are bigger compared to STHdh cells (nuclei of myoblasts measure ~ 15–20 μm whereas nuclei of STHdh cells measure <10 μm). This allows us to better evaluate the skeleton of the mitochondrial network. Our data showed that HD myoblasts displayed an increased percentage of class I and decreased percentage of class III as compared to control myoblasts. An extensive fragmentation (Class I) was observed in 37.5% of HD cells, 50% of cells contained short rods in addition to mitochondrial spheres (Class II) and only 12.5% of cells contained

medium−length tubules (Class III), whereas only 12.5% of control myoblasts contained completely fragmented mitochondria (Class I) (Fig. 8b shows mean±SEM; chi−square test, $p<0.01$).

Reduced ATP synthesis and oxygen consumption in STHdh cells.

STHdh cells were exposed to mild metabolic stress and nucleotides in cellular extracts were measured by HPLC analysis in order to quantify mitochondrial ATP production. Data were normalized on cell number assessed by Coulter Counter assay. ATP concentration in STHdhQ111/Q111 was decreased by 62% compared to STHdhQ7/Q7 cells (Fig. 9a-b. Fig. 9b represents mean±SEM deriving from four independent experiments; *$p< 0.05$).
We measured oxygen consumption in STHdh cells using a Clark−type polarographic oxygen electrode. A total of 10^6 cells were maintained in suspension in oxygen electrode buffer at 33° C throughout each experiment. We observed that STHdhQ111/Q111 cells have significantly reduced oxygen consumption rate (OCR) (6.125±0.79 nmol O_2/min/10^6 cells) compared with wild−type cells. (8.996±0.93 nmol O_2/min/10^6 cells) (Fig. 10 represents mean±SEM deriving from six independent experiments; *$p< 0.05$).

BNip3ΔTM expression improves mitochondrial membrane potential and restores normal mitochondrial morphology in human HD myoblasts.

As BNip3 integration into the OMM can elicit the reduction of $\Delta\psi_m$ on various toxic stimuli (Lee and Paik, 2006), we hypothesized that the high BNip3 levels we found associated with mitochondrial membrane fractions in HD cells could cause a decrease in $\Delta\psi_m$, previously observed in HD myoblasts and other HD models (Sawa *et al*., 1999; Ciammola *et al*., 2006; Benchoua *et al*., 2006; Bae *et al.,* 2005*).* In this context, we reasoned that blocking both BNip3 integration in the OMM and BNip3 dimerization by overexpression of the dominant-negative protein BNip3ΔTM would protect cells from the mitochondrial depolarization induced by mhtt. The mutant BNip3ΔTM lacks the C-terminal domain essential for integration into the OMM and has been shown to function as a dominant-negative mutant that blocks BNip3 translocation and integration into the OMM (Hamacher-Brady *et al*., 2007; Kubasiak *et al*., 2002). In human HD myoblasts, transient transfection with BNip3ΔTM did not modify mitochondrial $\Delta\psi_m$ both in control and HD myoblasts (data not shown), probably because of high endogenous levels of BNip3 and the low transfection efficiency of plasmid DNA in primary myoblasts (~60% of cells displayed green fluorescence 24 hours after trasfection with the pEGFP vector). However, co-transfection of cells with BNip3ΔTM

and with short interfering RNA (siRNA) to knock down endogenous BNip3 resulted in an efficient silencing of the endogenous protein (by ~70%, Fig. 11a), in a detectable expression of BNIP3ΔTM, as well as in a significant increase in $\Delta\psi_m$ in all four HD lines transfected (mean value 124%, **p<0.01; Fig. 11b). Overall, these results suggest that the $\Delta\psi_m$ loss in HD myoblasts may stem from BNip3 activation and that BNip3ΔTM expression resulted after 24 hours in a significant increase in $\Delta\psi_m$. Overexpression of the mutant protein BNip3ΔTM and silencing of endogenous BNip3 protect HD myoblasts from the mitochondrial depolarization induced by mutant htt.
We next verified whether the overexpression of BNip3ΔTM protein could normalize mitochondrial morphology in HD human myoblasts. We co-transfected myoblasts from 3 HD patients (CAG repeat on the upper allele were 59, 50 and 50) and 3 healthy controls with pDsRed2–Mito and with pBNip3ΔTM and 24 hours after transfection we analyzed mitochondrial morphology according to the above described criteria. For each subject 300 cells were randomly chosen and scored into the three categories. HD cells designated as class I lowered from 37.5% to 10%, whereas class II and class III percentage respectively increased from 50% to 66.7% and from 12.5% to 23.3% (Fig. 11c; chi–square test, p<0.01).Therefore the expression of BNip3ΔTM was able to restore mitochondrial elongation in HD myoblasts without causing any changes in mitochondrial morphology in control myoblasts.

BNip3ΔM expression restores normal mitochondrial morphology and improves mitochondrial function in STHdhQ111/111 cells.

We cotransfected STHdh cells with pDsRed2–Mito and pBNip3ΔTM and 3 days after transfection we analyzed mitochondrial morphology according to the above described criteria. BNip3ΔTM overexpression striking decreased the mitochondrial fragmentation observed in mutant cells, leading to an increase of mitochondrial medium–length tubules in STHdhQ111/Q111 cells from 19.25% to 33.5% (Fig. 12a; chi–square test, p<0.05). Figure 12b shows as STHdhQ111/111 cells has similar mitochondrial phenotype 6 days after transfection (p<0.05).
We also measured JC–1 ratio in the STHdh cells transiently transfected with BNip3ΔTM for three days. We observed that overexpression of BNip3ΔTM in wild–type cells didn't modify JC–1 ratio whereas BNip3ΔTM significantly increased JC–1 ratio in STHdhQ111/111 cells (Fig 12c; *p<0.05), without altering the mitochondrial mass content (data not shown).
Although BNip3ΔTM overexpression for 3 days improves mitochondrial membrane potential in STHdhQ111/111 cells, we observed also that its overexpression wasn't able to increase ATP level in the same cells (Fig 12d).
Finally, we analyzed oxygen consumption in STHdh cells. We observed that 3 days or 6 days of overexpression of BNip3ΔTM in STHdhQ111/Q111 didn't increase the oxygen consumption rate

(Fig. 12e-f). We repeated these measurements also after 11 days of expression of BNip3ΔTM. To maintain high the level of the transgene we have repeated the transfection on the sixth day and then we have verified its expression by Western blot analysis. Our results demonstrated that BNip3ΔTM causes a mild improvement in the oxygen consumption rate in STHdhQ111/Q111 cells (Fig 12g).

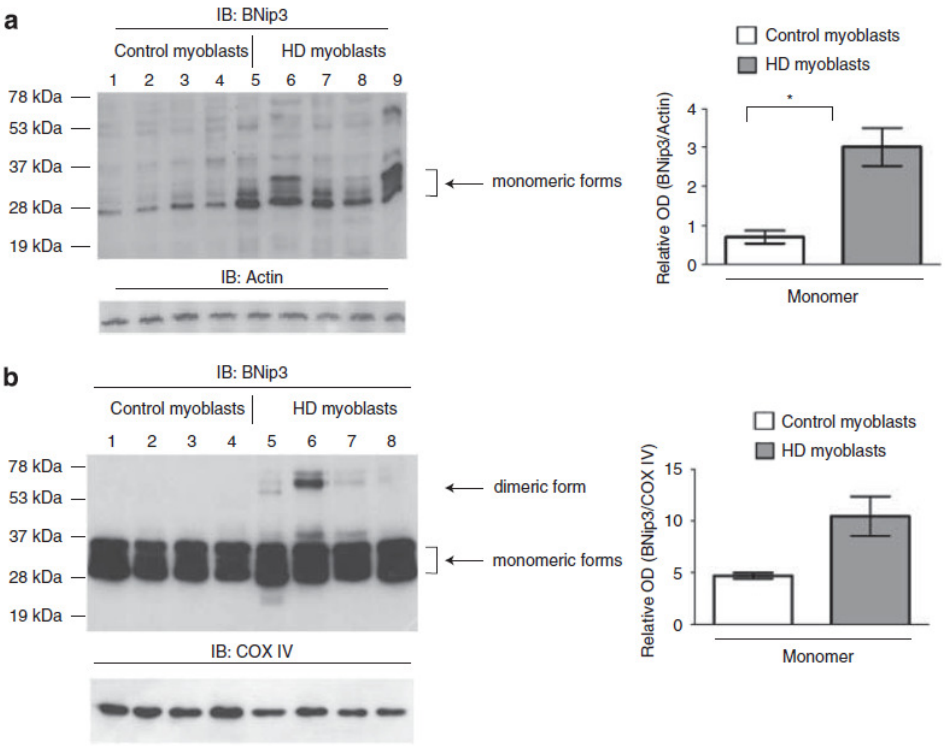
a
IB: BNip3
Control myoblasts
HD myoblasts
1 2 3 4 5 6 7 8 9
78 kDa
53 kDa
37 kDa
28 kDa
19 kDa
monomeric forms
IB: Actin
Control myoblasts
HD myoblasts
Relative OD (BNip3/Actin)
Monomer
b
IB: BNip3
Control myoblasts
HD myoblasts
1 2 3 4 5 6 7 8
78 kDa
53 kDa
37 kDa
28 kDa
19 kDa
dimeric form
monomeric forms
IB: COX IV
Control myoblasts
HD myoblasts
Relative OD (BNip3/COX IV)
Monomer

c

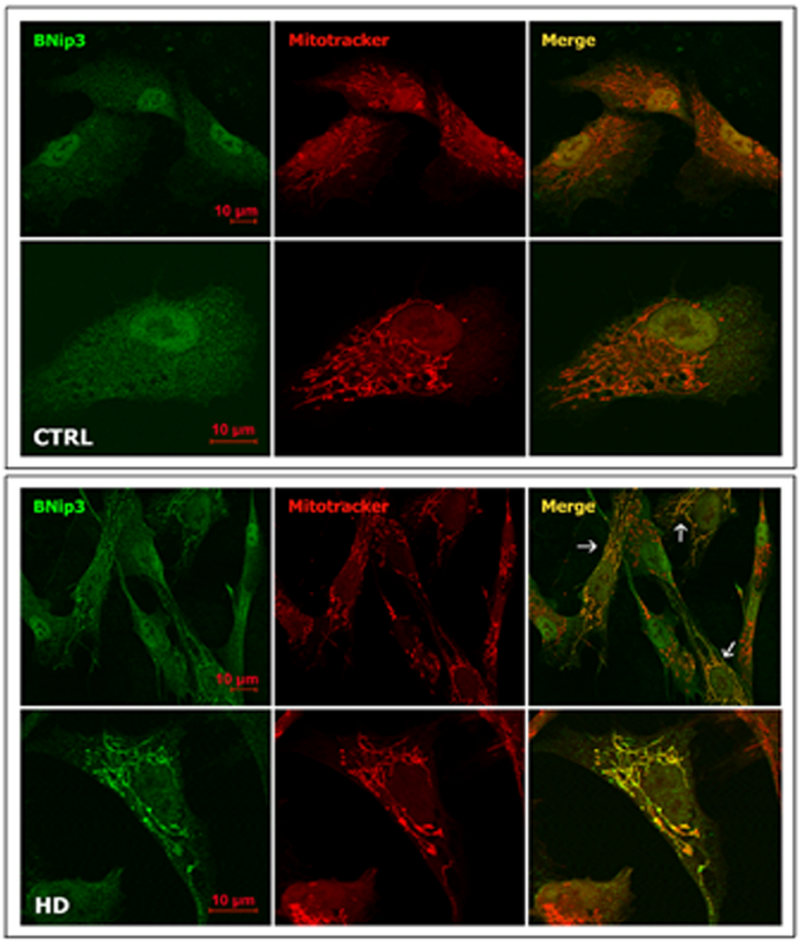

Fig. 1. Analysis of BNip3 expression and BNip3 integration into the mitochondrial membranes of human myoblasts. **(a)** Equal protein amounts from control and HD myoblasts were analyzed by WB and probed with anti-BNip3 antibody. The signal corresponding to monomeric BNip3 was higher in HD myoblasts (from left to right: 42 CAG, 42 CAG, 60 CAG and 48 CAG) than in control myoblasts. Actin was used as a loading control Protein band densitometry is reported in the corresponding graphs as means±SEM (* p<0.05). **(b)** Mitochondria-enriched fractions from control and HD myoblasts were analyzed by WB. Protein band densitometry is reported in the corresponding graphs as means±SEM. Dimeric BNip3 signal was clearly detectable in HD myoblasts (from left to right: 48 CAG, 60 CAG, 42 CAG and 42 CAG, * p<0.05). **(c)** Confocal microscopy on control and HD (60 CAG) myoblasts. White arrows indicate regions of extended BNip3 and mitochondrial co-localization in HD myoblasts. The image is representative of four myoblast cultures from four HD patients.

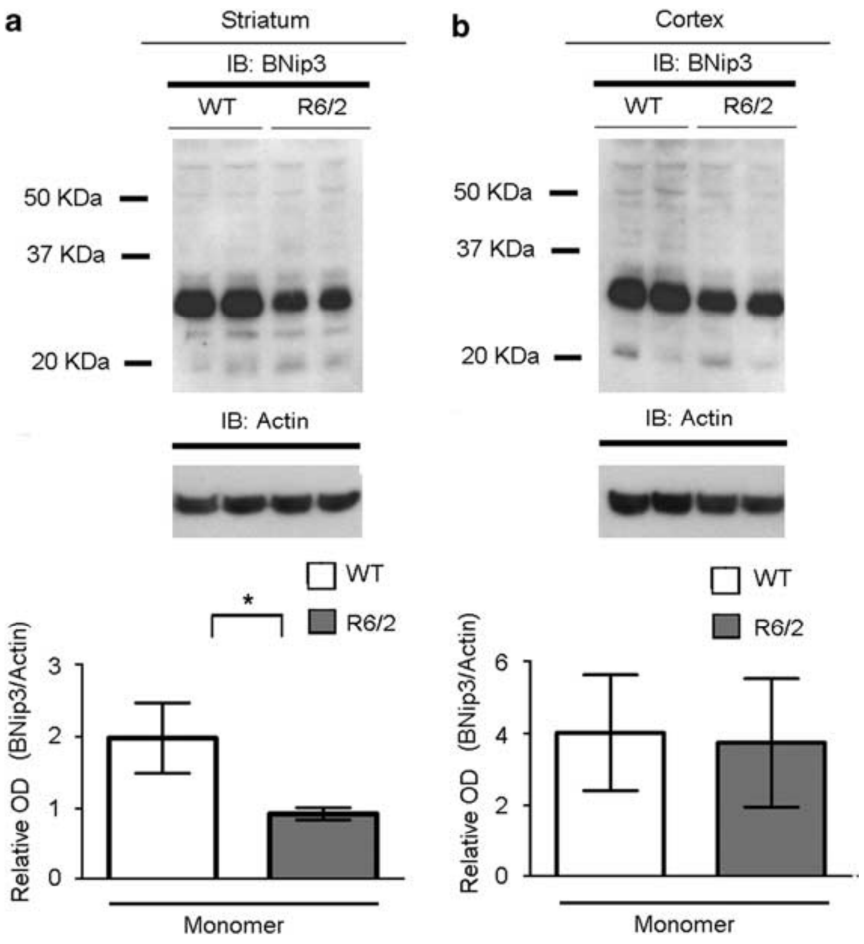
a
Striatum
IB: BNip3
WT
R6/2
50 KDa
37 KDa
20 KDa
IB: Actin
WT
R6/2
*
Relative OD (BNip3/Actin)
3
2
1
0
Monomer
b
Cortex
IB: BNip3
WT
R6/2
50 KDa
37 KDa
20 KDa
IB: Actin
WT
R6/2
Relative OD (BNip3/Actin)
6
4
2
0
Monomer

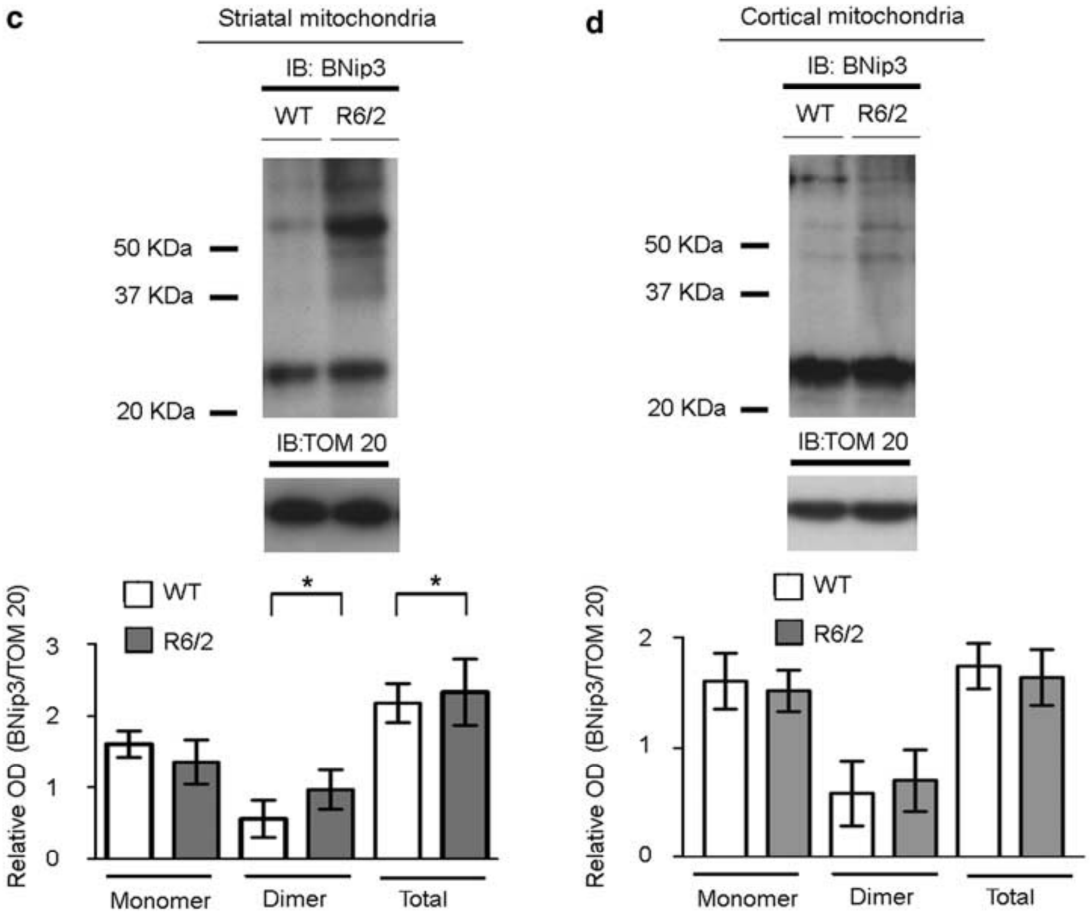
c
Striatal mitochondria
IB: BNip3
WT R6/2
50 KDa
37 KDa
20 KDa
IB:TOM 20
WT
R6/2
*
*
Relative OD (BNip3/TOM 20)
0
1
2
3
Monomer
Dimer
Total
d
Cortical mitochondria
IB: BNip3
WT R6/2
50 KDa
37 KDa
20 KDa
IB:TOM 20
WT
R6/2
Relative OD (BNip3/TOM 20)
0
1
2
Monomer
Dimer
Total

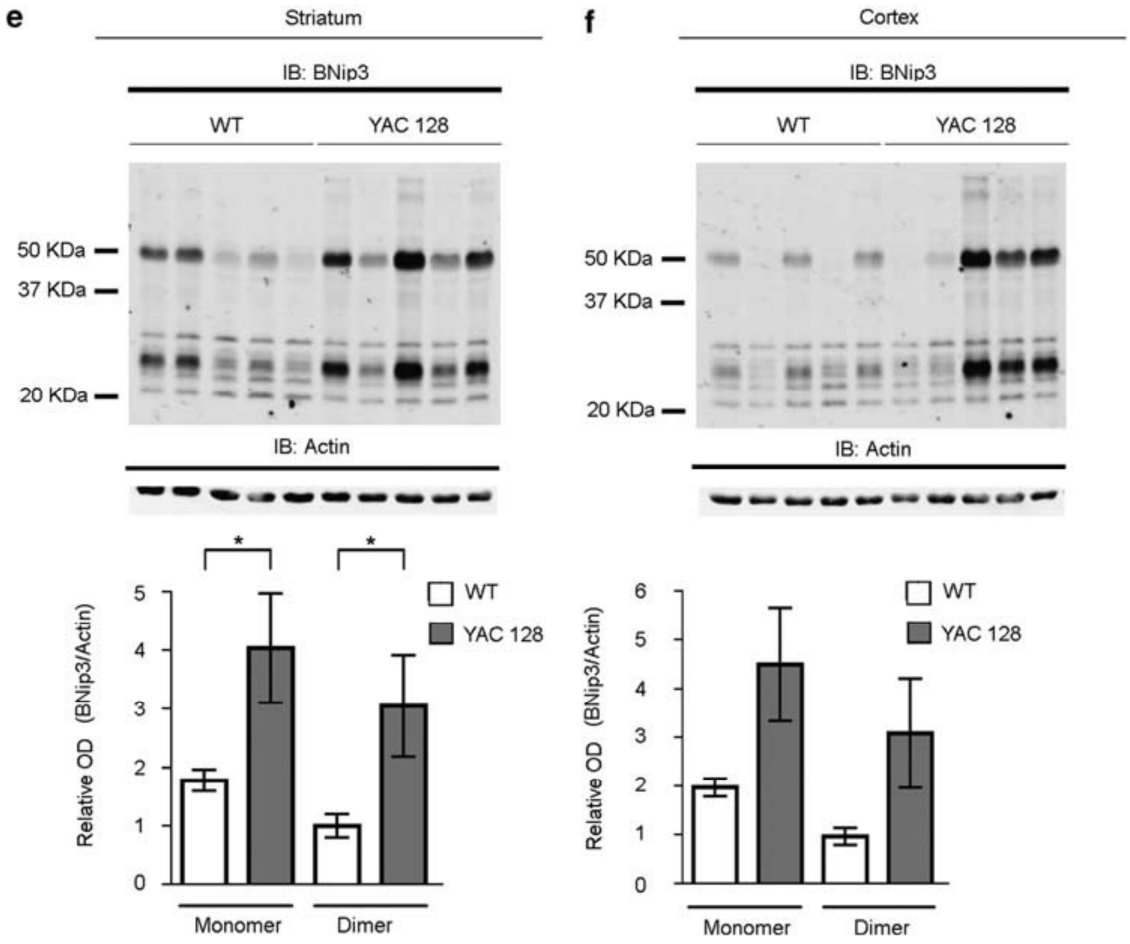
e
Striatum
IB: BNip3
WT
YAC 128
50 KDa
37 KDa
20 KDa
IB: Actin
Relative OD (BNip3/Actin)
WT
YAC 128
Monomer
Dimer
f
Cortex
IB: BNip3
WT
YAC 128
50 KDa
37 KDa
20 KDa
IB: Actin
Relative OD (BNip3/Actin)
WT
YAC 128
Monomer
Dimer

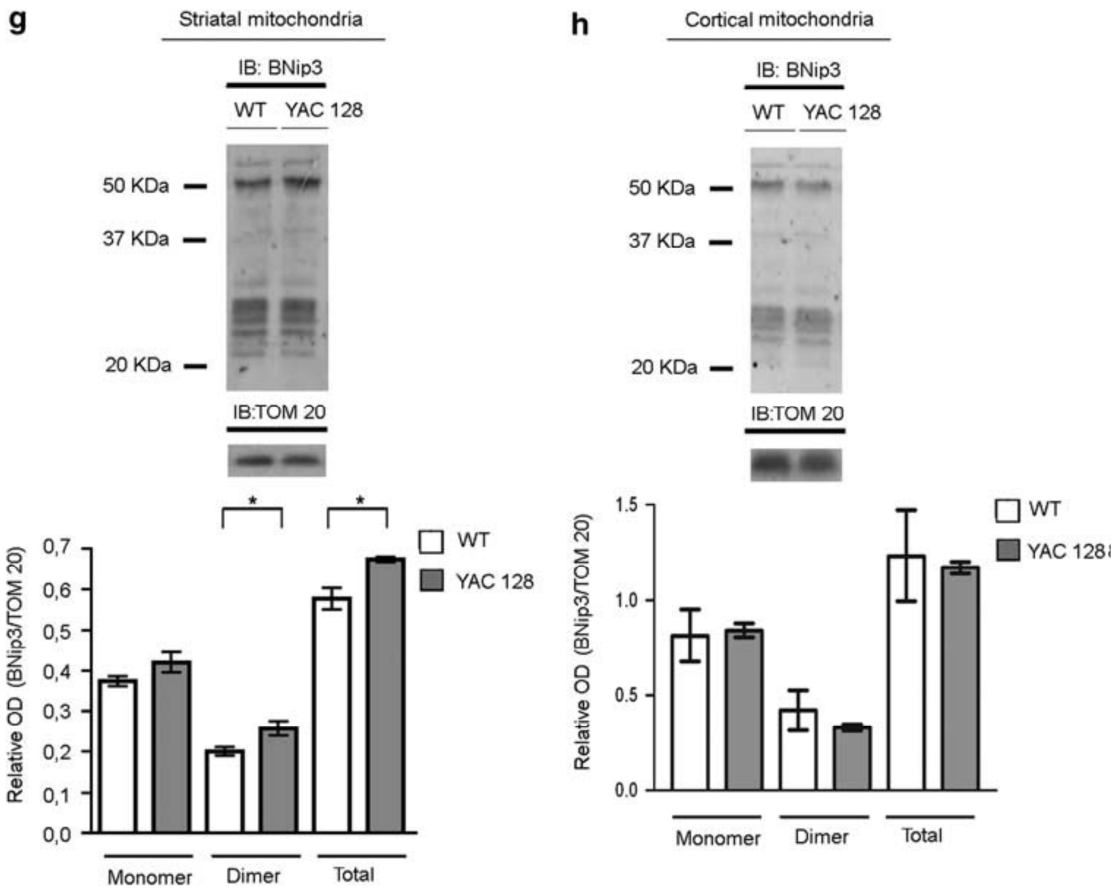

Fig. 2. Analysis of BNip3 level and BNip3 integration into the mitochondrial membrane in the brains of R6/2 and YAC128 mice. (a-b) Whole protein lysates of striatum and cortex from 10-week-old R6/2 and littermate control mice were analyzed by WB, using anti-BNip3 antibodies. There was a trend of decreasing monomeric BNip3 in R6/2 striatum (* $p<0.05$). No statistically significant difference in total BNip3 expression between R6/2 and wild-type mice was detected in cortical tissues. Data are representative of 6 R6/2 and 6 wild-type mice. **(c-d)** The panels show WB analysis of alkali-treated mitochondrial fractions from the striata and cortexes of 10-week-old R6/2 and control mice. To verify equal protein loading, the membranes were stripped and reprobed with anti-TOM20 antibody. Data are representative of six R6/2 and six wild-type mice analyzed (* $p<0.05$). **(e-f)** Immunoblotting and densitometric analysis of BNip3 expression in total lysates from striatum and cortex samples of five 6-month-old YAC128 mice and control littermates. Each lane represents one individual animal. Protein band densitometry results are reported in the corresponding graphs as means±SEM (two-tailed *t*-test, * $p<0.05$). **(g-h)** The panels show immunoblotting and densitometric analysis of BNip3 in alkali-treated mitochondrial fractions from striata and cortexes of YAC128 and control mice. TOM20 was used as a loading control (two-tailed *t*-test, * $p<0.05$).

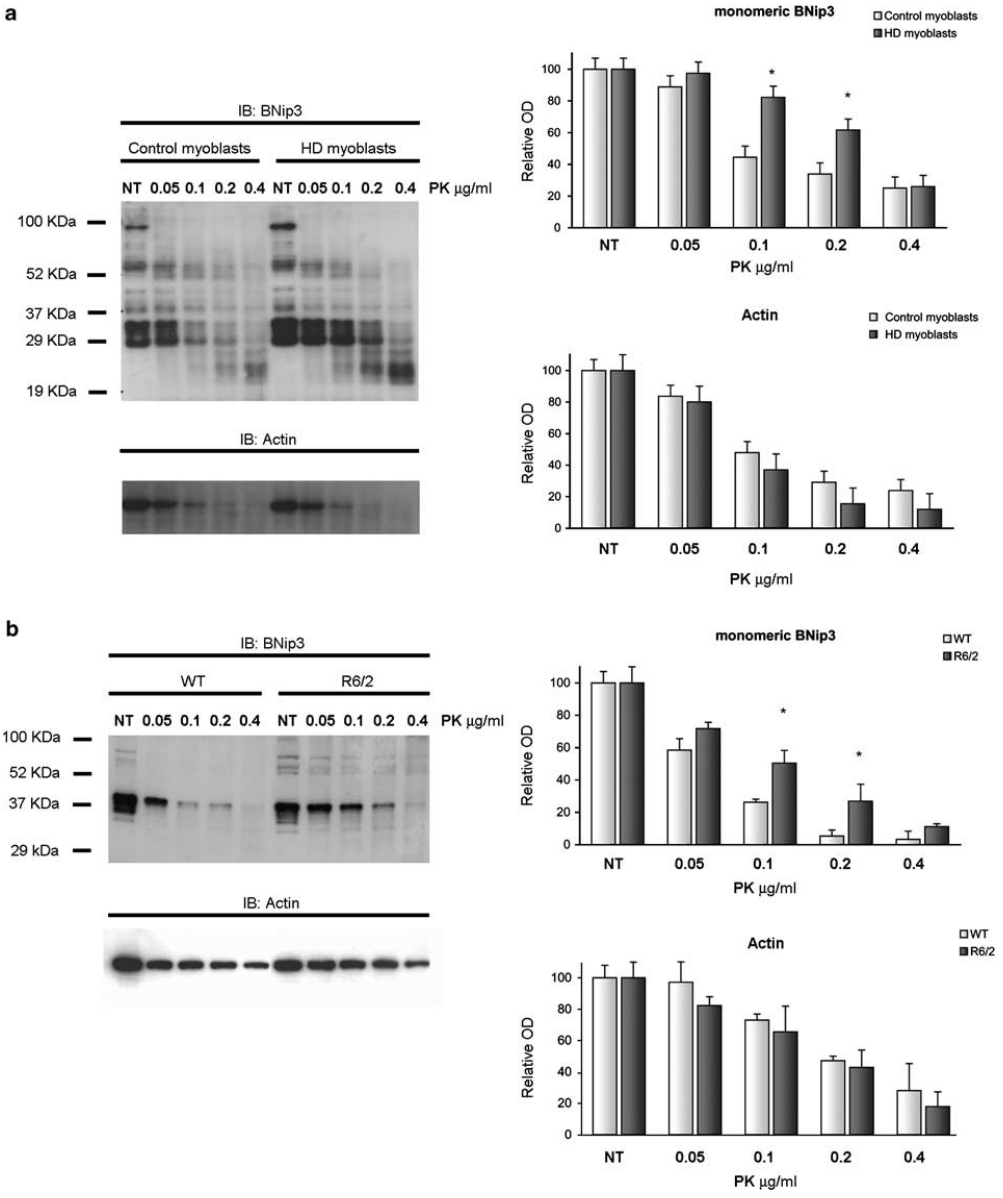

Fig. 3. Increased resistance of monomeric BNip3 to proteinase-K digestion in HD cells. Total cell extracts from four human myoblasts **(a)** and three R6/2 mouse brains **(b)** were digested in vitro for 8 min with increasing concentrations of PK. Lysis buffer contained 20 mM Tris (pH 7.5), 150 mM NaCl, 1 mM EDTA, 1% Triton X-100, 1 µg/ml pepstatin, 1 µg/ml leupeptin and 20 µM MG132. Densitometric analysis was performed on monomeric BNip3 signals. Multiple bands corresponding to monomeric forms were analyzed together. Data are reported as means±SEM, as percentages of the untreated sample. Monomeric BNip3 extracted from HD samples demonstrated increased resistance to PK digestion (* $p<0.05$ versus control sample). No difference in actin digestion patterns was detected between HD and control samples.

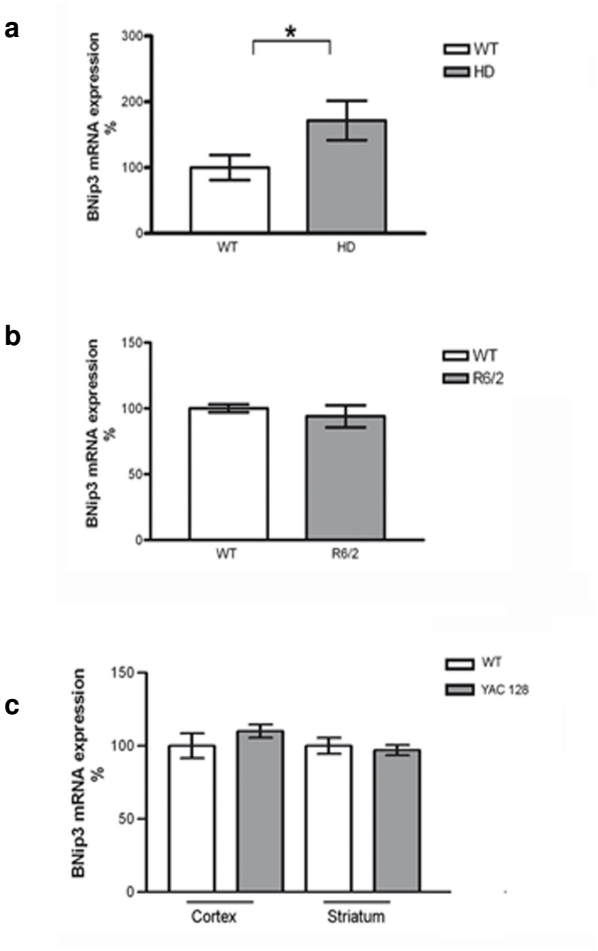

Fig. 4. Quantitative analysis of BNip3 mRNA. BNip3 mRNA was extracted from **(a)** human HD and control myoblasts, **(b)** R6/2 and control brains, **(c)** YAC128 and control brains. The level of each mRNA was normalized to that of cyclophilin A and actin. Data are presented as means±SEM (* $p<0.01$).

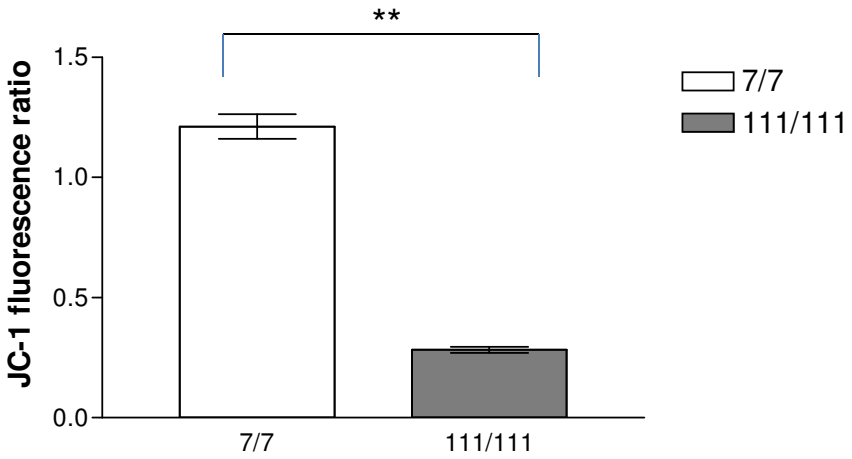

Fig. 5. Analysis of JC-1 fluorescence ratio in STHdhQ7/Q7 and STHdhQ111/Q111 cells. JC–1 is a mitochondrial dye that stains mitochondria in living cells in a membrane potential–dependent fashion. JC–1 monomer is in equilibrium with so–called J–aggregates, which are favored at higher mitochondrial membrane potential. The monomer JC–1 has green fluorescence (em = 527 nm), while the J–aggregates have red fluorescence (em = 590 nm). JC–1 ratio is used to measure the $\Delta\psi_m$. JC–1 ratio was measured in STHdh cells maintained in mild metabolic stress condition for three days. We observed that $\Delta\psi_m$ was decreased by ~ 70% in STHdhQ111/Q111 cells compared to STHdhQ7/Q7 (Data derive from six independent experiments. Fig. 5; **p< 0.01).

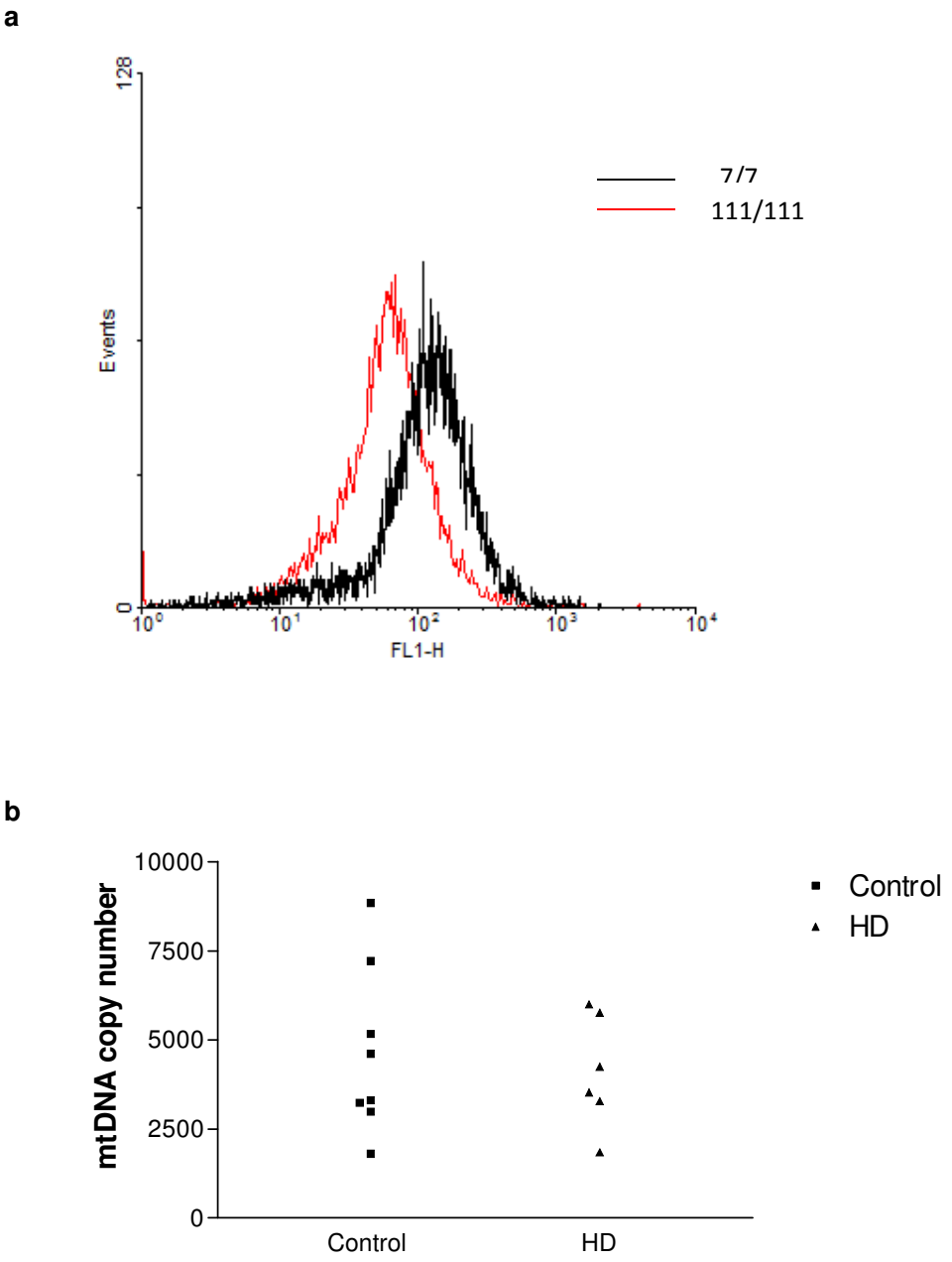

Fig. 6. Analysis mitochondrial content in HD cells. (a) Representative histogram obtained from STHdhQ7/Q7 and STHdhQ111/Q111 cells loaded with MitoTracker Green FM using flow cytometry. MitoTracker Green FM is a non-potentiometric fluorescent probe that stains mitochondria and its fluorescence is a measure of mitochondrial mass. STHdhQ111/Q111 cells have a reduced mitochondrial mass content compared to control cells. **(b)** Relative mtDNA content from myoblasts obtained from 8 control subjects and 6 HD patients. A difference was observed between control and HD myoblasts, but it is not statistically significant.

a

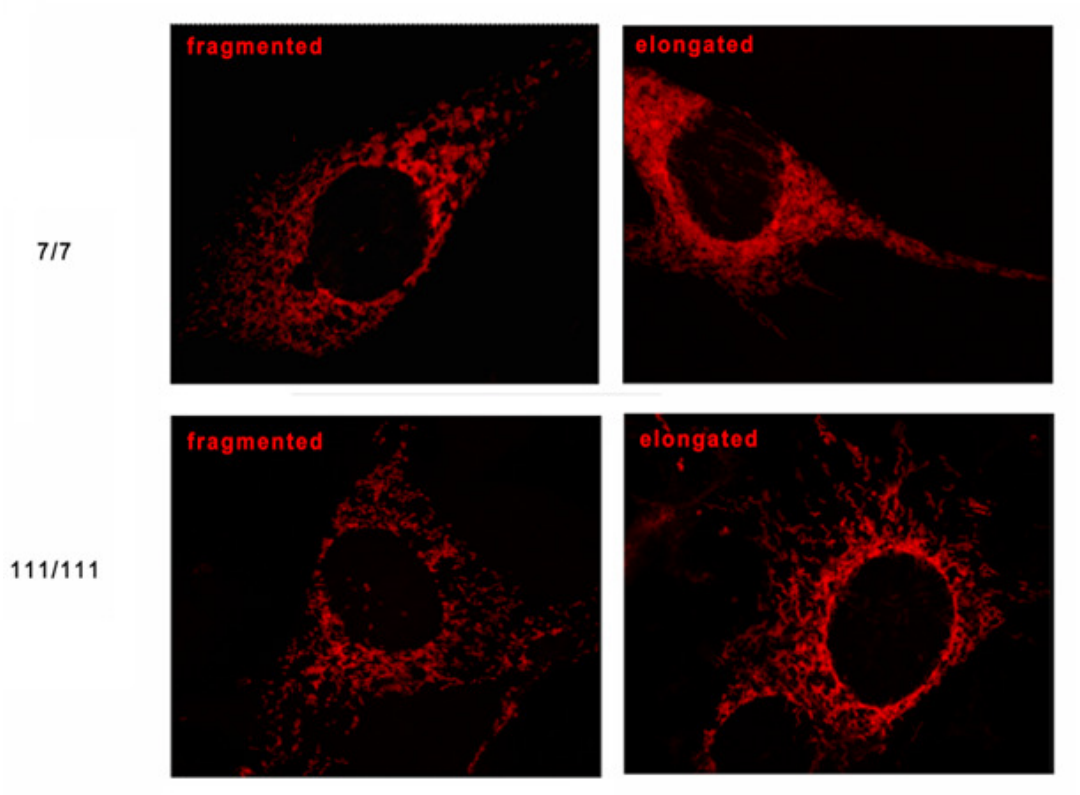

b

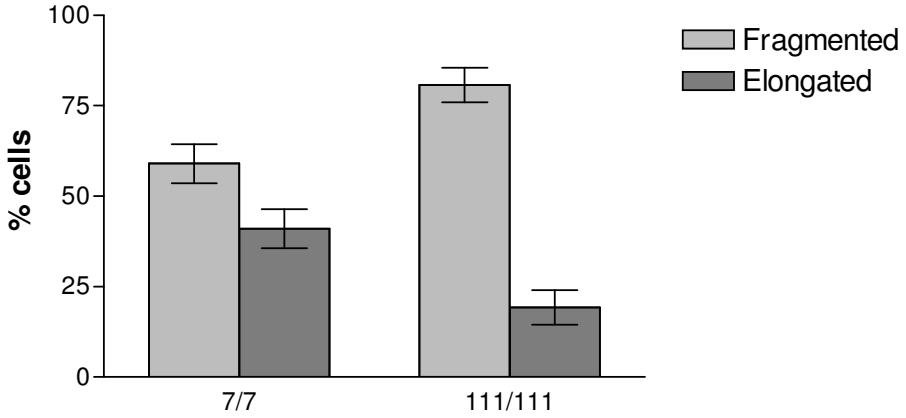
100
75
50
25
0
% cells
7/7
111/111
Fragmented
Elongated

c

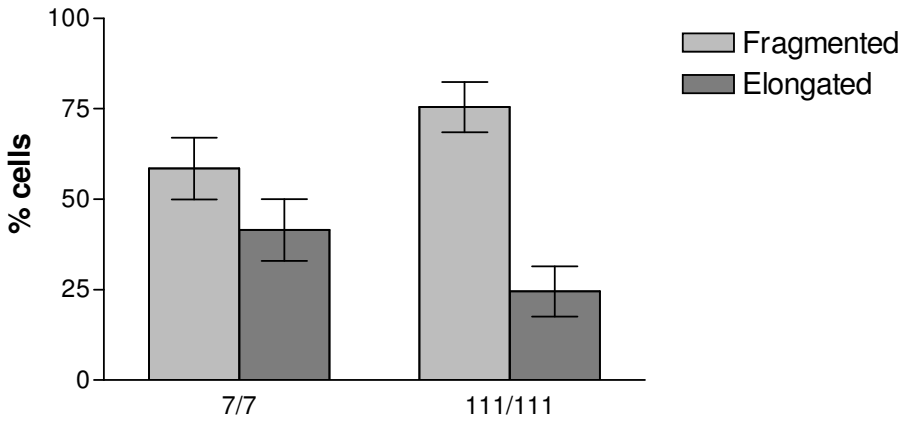
100
75
50
25
0
% cells
7/7
111/111
Fragmented
Elongated

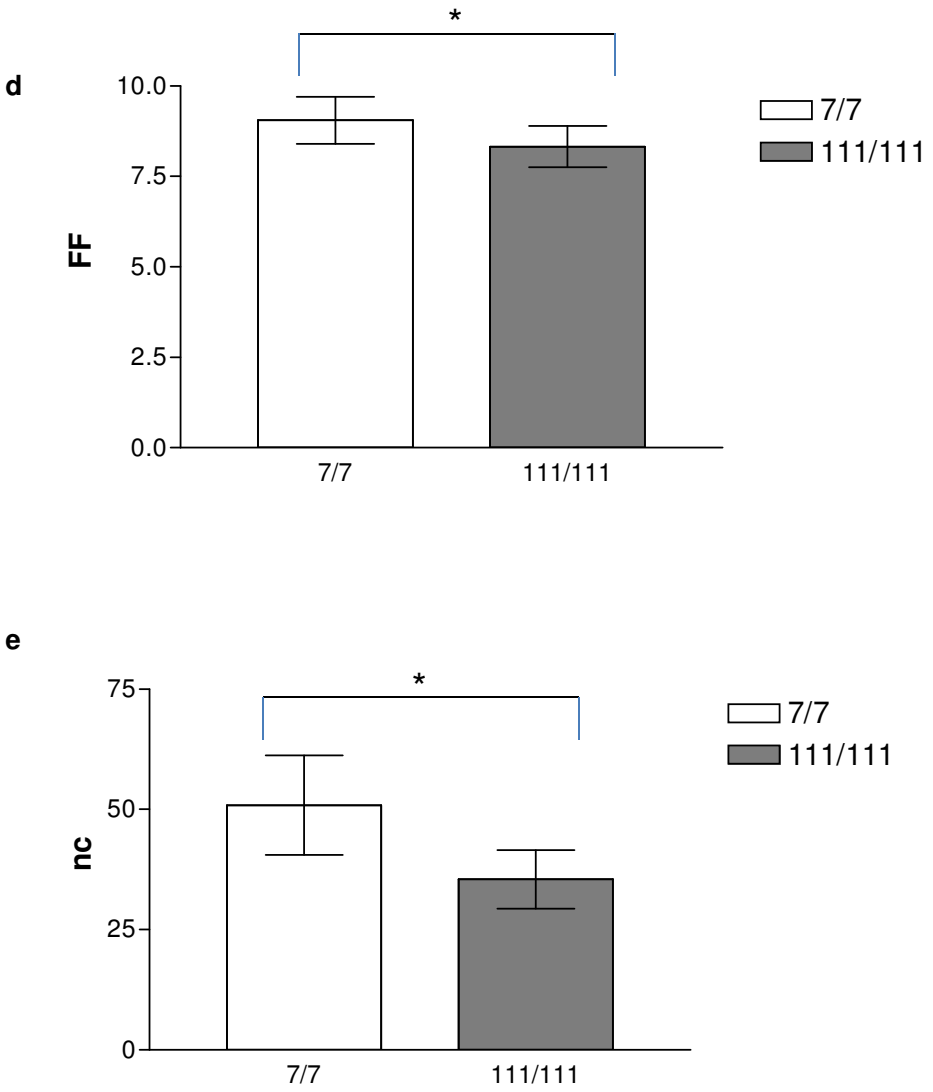

Fig. 7. Analysis of mitochondrial morphology in STHdhQ7/Q7 and STHdhQ111/Q111 cells. (a) Confocal image of DsRed protein-labeled mitochondria in STHdhQ7/Q7 and STHdhQ111/Q111 cells cultured for 3 days with mild metabolic strees medium. The images are representative of cells with fragmented and elongated mitochondria. Bar graph showing differences in mitochondrial morphologies in STHdhQ7/Q7 and STHdhQ111/Q111 cells after 3 **(b)** (chi-square test, $p<0.01$) or 6 days **(c)** (chi-square test, $p<0.05$) of treatment in galactose medium. 400 cells were counted for each condition. Data are presented as means±SEM. Computer-assisted quantitative analyses of mitochondrial morphology obtained using ImageJ 1.42 softare. FF is an indicator of mitochondrial length and branching, nc represents the number of mitochondria. STHdhQ111/Q111 cells displayed a slight decrease in FF **(d)** and nc **(e)** compared to STHdhQ7/Q7 cells. Data are presented as means±SEM (* $p<0.05$).

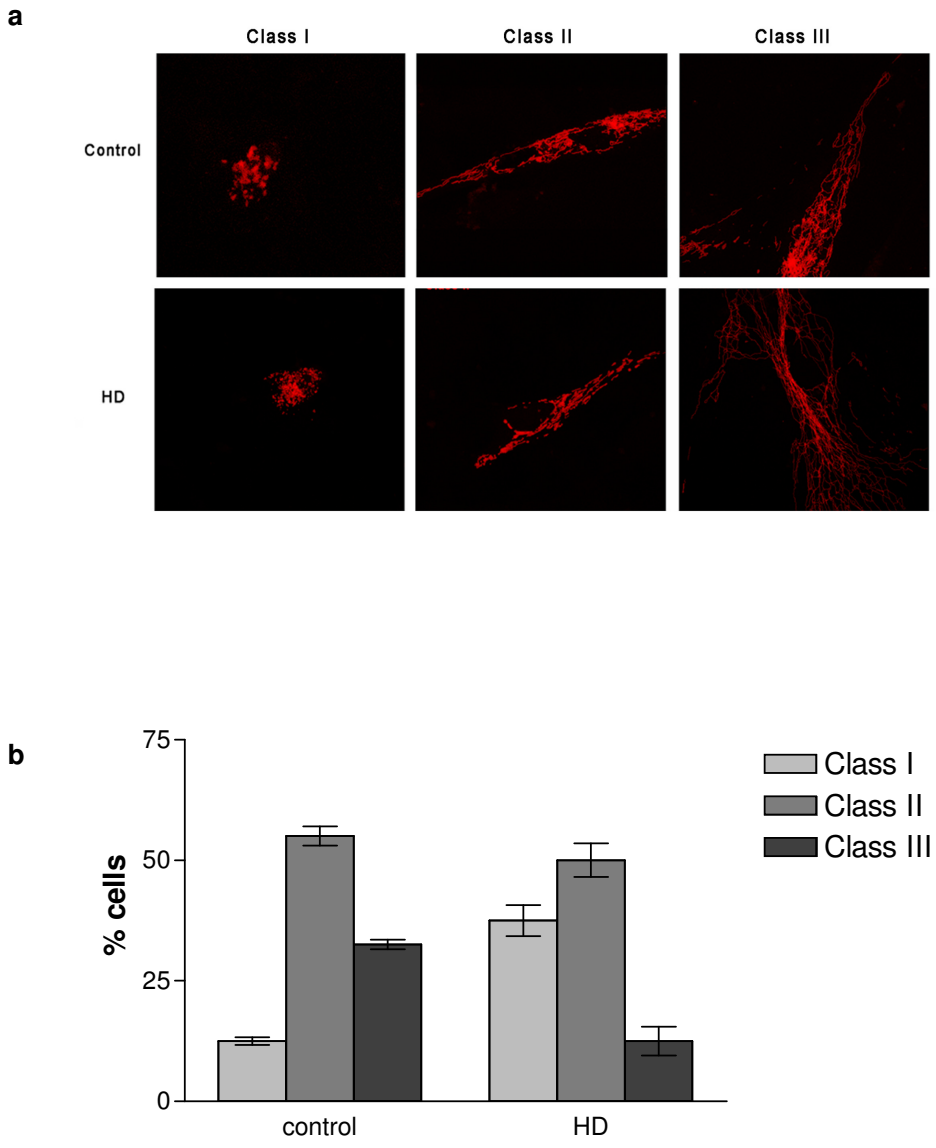

Fig. 8. Analysis of mitochondrial morphology in myoblasts obtained from human subjects. (a) Representative confocal image of DsRed protein-labeled mitochondria in control and HD myoblasts. **(b)** Bar graph showing differences in mitochondrial morphologies. 300 cells were counted for each subject (3 control and 3 HD myoblasts). Data are presented as means±SEM (chi-square test, $p<0.01$).

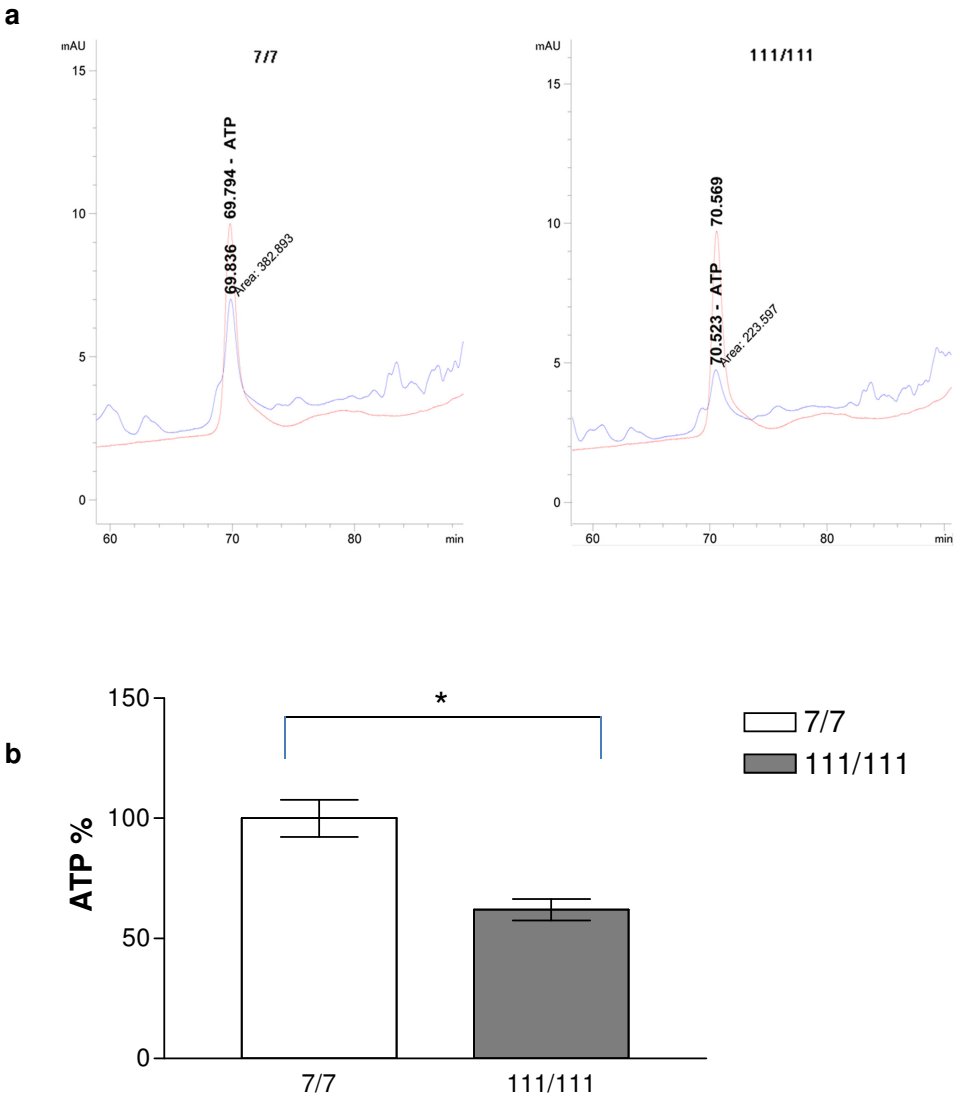

Fig. 9. Analysis of ATP production in STHdh cells. (a) HPLC chromatograms of ATP in STHdhQ7/Q7 and STHdhQ111/Q111 cells. **(b)** Bar graph showing differences in ATP concentrations in STHdh cells after 3 days in mild metabolic stress medium. Data are presented as % means±SEM (*p<0.05).

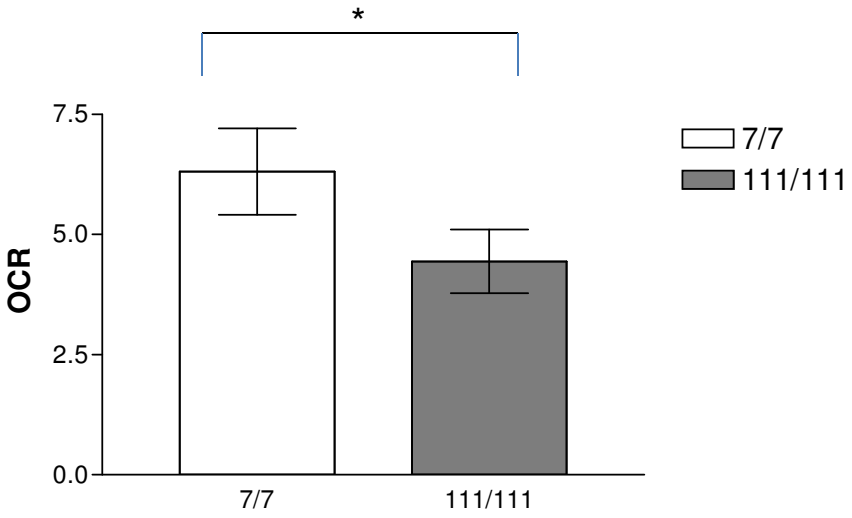

Fig. 10. Analysis of oxygen consumption in STHdh cells. Bar graph showing oxygen consumption rate (OCR) in STHdhQ7/Q7 (8.996± 0.93 nmol/O_2/10^6 cells) and STHdhQ111/Q111 cells (6.125± 0.79 nmol/O_2/10^6 cells) after 3 days in mild metabolic stress medium. Data are presented as means±SEM (*p<0.05).

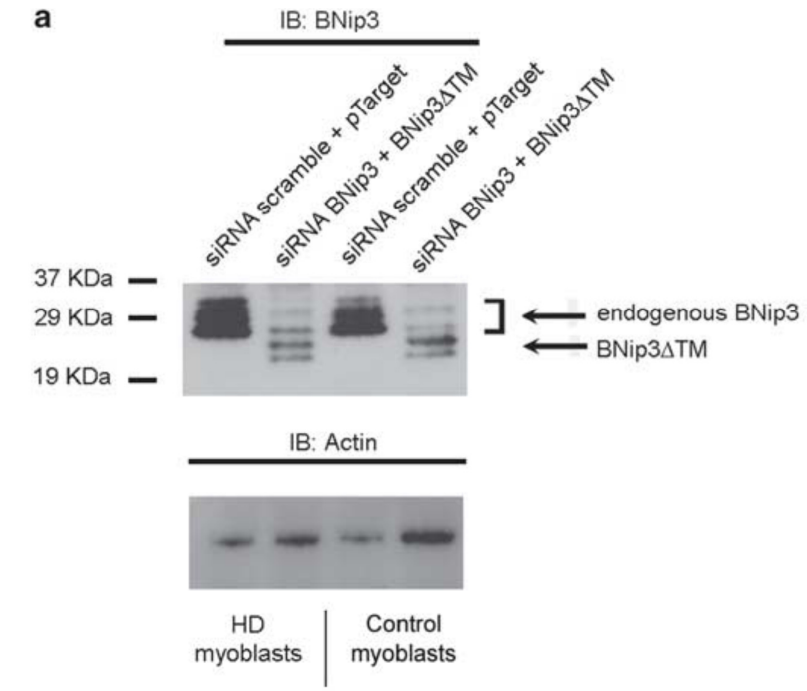
a
IB: BNip3
siRNA scramble + pTarget
siRNA BNip3 + BNip3ΔTM
siRNA scramble + pTarget
siRNA BNip3 + BNip3ΔTM
37 KDa
29 KDa
19 KDa
endogenous BNip3
BNip3ΔTM
IB: Actin
HD myoblasts
Control myoblasts

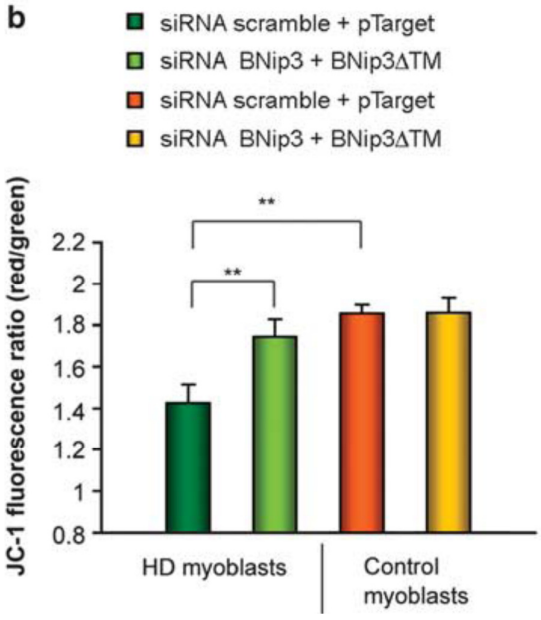
b
siRNA scramble + pTarget
siRNA BNip3 + BNip3ΔTM
siRNA scramble + pTarget
siRNA BNip3 + BNip3ΔTM
JC-1 fluorescence ratio (red/green)
2.2
2
1.8
1.6
1.4
1.2
1
0.8
**
**
HD myoblasts
Control myoblasts

c

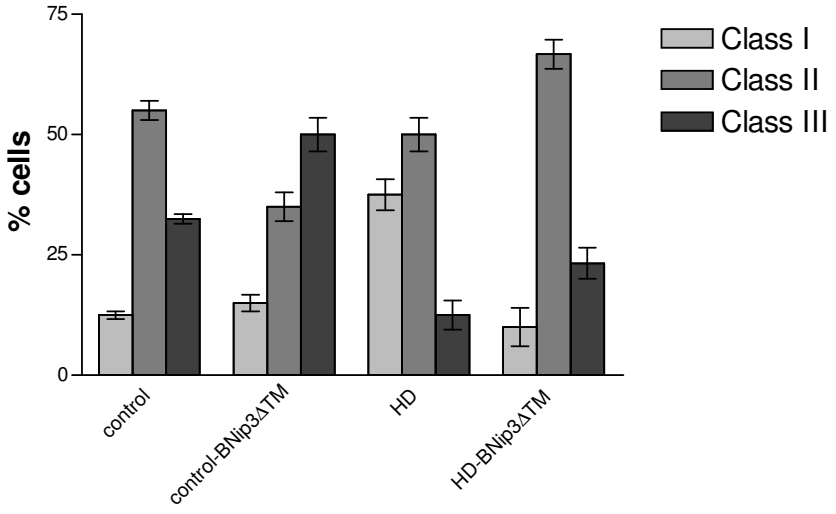

Fig. 11. BNip3ΔTM overexpression improves mitochondrial function and morphology. (a) WB analysis of co-transfected myoblasts. **(b)** Analysis of $\Delta\psi_m$ in human HD (4 samples) and control (4 samples) myoblasts, after treatment with siRNA against BNip3 together with a plasmid encoding BNip3ΔTM. Data are presented as means±SEM (** $p<0.01$). Cultured cells were transfected with equal total amounts of plasmid DNA. **(c)** Bar graph showing differences in mitochondrial morphologies in myoblasts transfected with empty vector or BNip3 ΔTM. 300 cells were counted for each subject (3 control and 3 HD myoblasts). Data are presented as means±SEM (chi-square test, $p<0.01$).

a

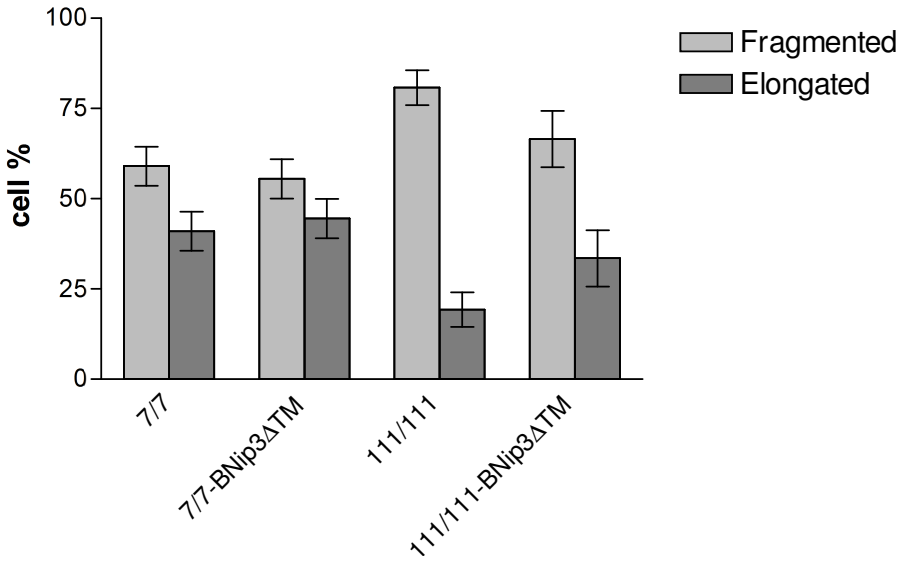
100
75
50
25
0
cell %
Fragmented
Elongated
7/7
7/7-BNip3ΔTM
111/111
111/111-BNip3ΔTM

b

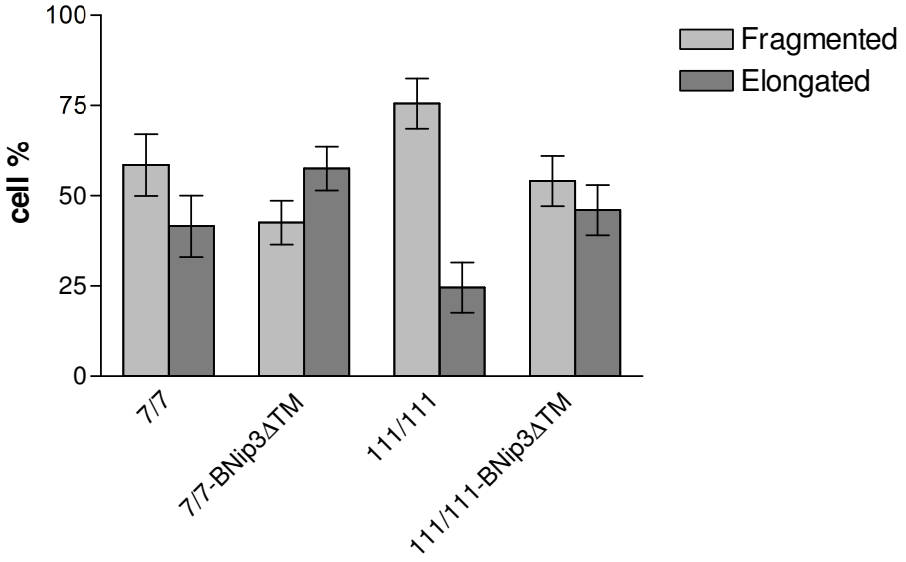
100
75
50
25
0
cell %
Fragmented
Elongated
7/7
7/7-BNip3ΔTM
111/111
111/111-BNip3ΔTM

c

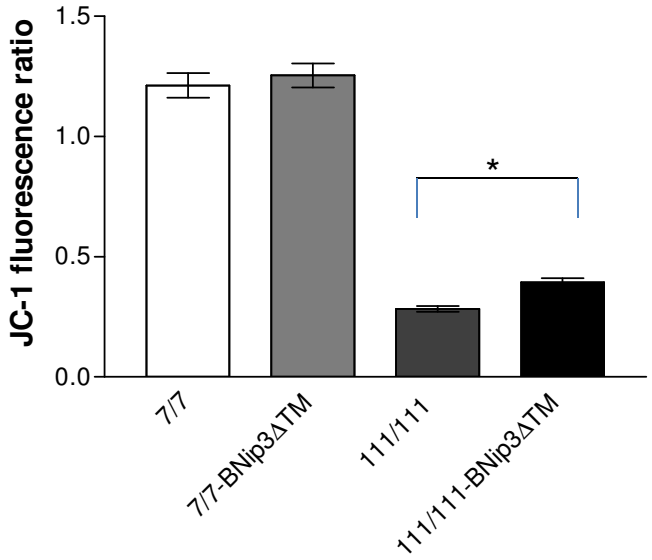
JC-1 fluorescence ratio
1.5
1.0
0.5
0.0
*
7/7
7/7-BNip3ΔTM
111/111
111/111-BNip3ΔTM

d

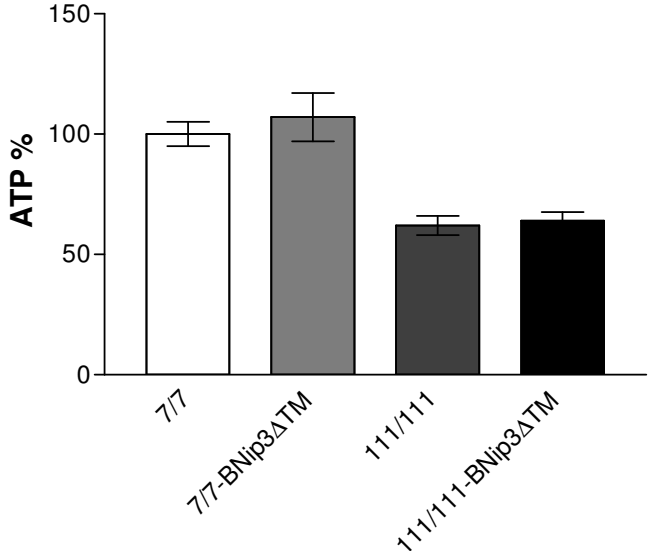
ATP %
150
100
50
0
7/7
7/7-BNip3ΔTM
111/111
111/111-BNip3ΔTM

e

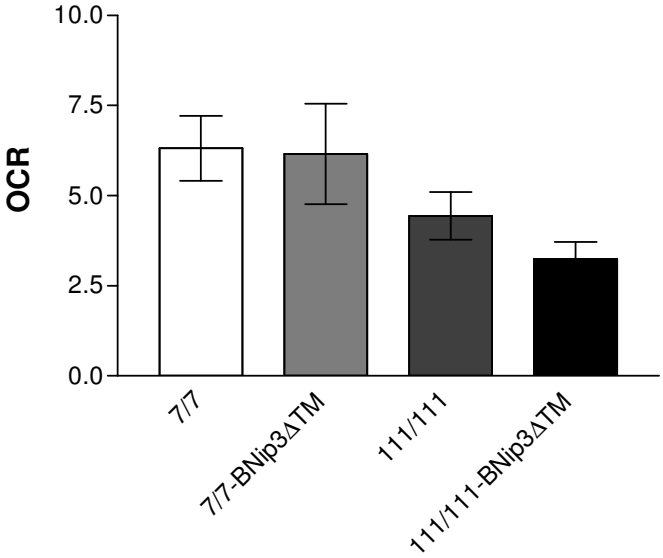
10.0
7.5
5.0
2.5
0.0
OCR
7/7
7/7-BNip3ΔTM
111/111
111/111-BNip3ΔTM

f

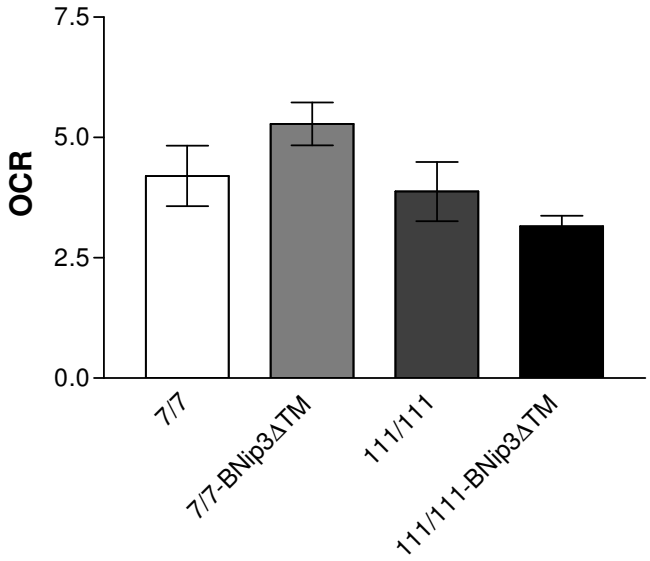
7.5
5.0
2.5
0.0
OCR
7/7
7/7-BNip3ΔTM
111/111
111/111-BNip3ΔTM

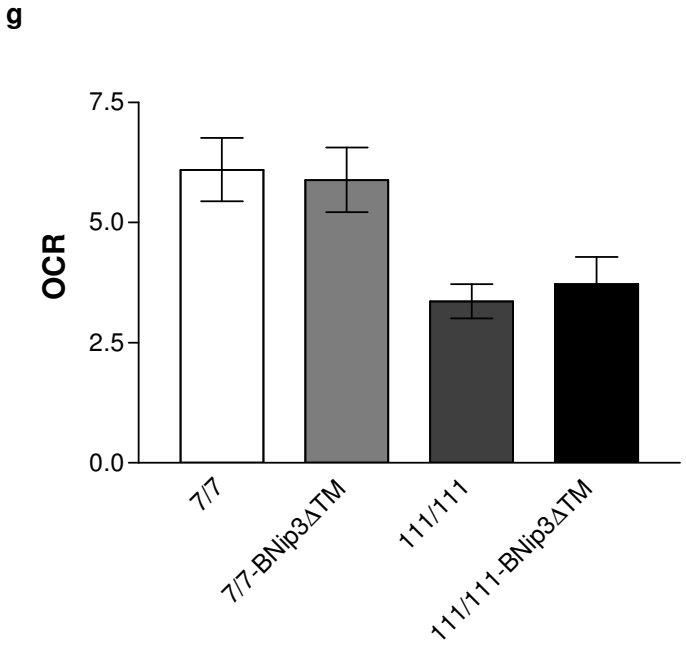

Fig. 12. BNip3ΔTM overexpression restores mitochondrial morphologyin STHdh cells cultured in mild metabolic stress medium. Bar graph showing differences in mitochondrial morphologies in transfected with empty vector or BNip3 ΔTM for 3 **(a)** or 6 **(b)** days . 400 cells were counted per group. Data are presented as means±SEM (chi-square test, $p<0.05$). **(c)** Analysis of $\Delta\psi_m$ in STHdhQ7/Q7 and STHdhQ111/Q111 cells 3 days after transfection with empty vector or BNip3 ΔTM. Data are presented as means±SEM (* $p<0.01$). **(d)** Bar graph showing differences in ATP concentrations in STHdh cells. Bar graph showing differences in oxygen consumption rate 3 **(e)** 6 **(f)** and 11 **(g)** after transfection with BNip3ΔTM in STHdh cells.

Conclusions and Future Prospects

Many years have passed since the discovery of the HD mutation (HDCRG, 1993), however, no therapy to date has shown a neuroprotective effect or has been shown to slow down disease progression, most likely because the precise pathophysiological mechanisms of HD are poorly understood. Growing evidence suggests that mitochondrial function is compromised during early phases of HD pathogenesis (Browne, 2008), but how mhtt damages mitochondria is not yet understood. Evidence that accrued over the past few years increasingly favors the hypothesis that mitochondrial dysfunction has a key function in the death of the neuronal cells of HD patients (Browne, 2008; Bossy-Wetzel *et al*., 2008). Nevertheless, the nature of such mitochondrial damage has remained elusive so far. Our results suggest a role of BNip3 protein in the mitochondrial dysfunction induced by mhtt. Clinical and experimental studies have provided convincing evidence that mitochondrial dysfunction occurs in the CNS and skeletal muscle tissue of HD patients (Saft *et al*., 2005; Browne, 2008; Arenas *et al*., 1998; Lodi *et al*., 2000). Thus, cultures of human myoblasts obtained from HD patients are an excellent model to study the pathogenic effects of mhtt on the mitochondria. A former study showed a pathological decrease of $\Delta\psi_m$ in HD myoblasts (Ciammola *et al*., 2006). In this study, we provide evidence that BNip3 levels are increased in total lysates of HD myoblasts. More importantly, we demonstrate that more BNip3 colocalized with the mitochondria in human HD myoblasts when compared with age-matched control myoblasts. The increased total level of the BNip3 protein might depend both on transcriptional and on post-transcriptional regulation. However, results indicating increased BNip3 translocation into the mitochondria and BNip3 integration into the OMM in HD cells suggest that post-transcriptional mechanisms are primarily involved. This hypothesis is further supported by the finding that the BNip3 protein in HD myoblasts is more resistant to PK digestion compared with that in control samples, probably because of the acquisition of an alternative conformation as a prelude to BNip3 activation (Frazier *et al*., 2006). The results obtained from human HD myoblasts were confirmed in the brain tissue extracted from two different animal models of HD, R6/2 and YAC128 mice. In both animal models, we observed increased levels of dimeric BNip3 associated with striatal mitochondrial fractions. Importantly, YAC128 mice showed increased BNip3 levels in the striatum at 6 months of age when, in spite of overt motor symptoms, no striatal tissue loss had yet occurred. This suggests that alterations in BNip3 localization and activity may precede neural loss in HD. Unfortunately, a study on BNip3 in human HD brains cannot be conducted, as BNip3 expression and activation are strongly induced by hypoxic conditions that inevitably precede the collection of autopsy specimens. A large number of studies using cell culture models have shown that BNip3 integration into the OMM leads to a potential loss of mitochondria (Vande Velde *et al*., 2000; Kim *et al*., 2002; Kubasiak *et al*., 2002; Kubli *et al*., 2007). In accordance with those results, a recent report described the spatial structure of BNip3 in a membrane-mimicking lipid environment,

showing that BNip3 homodimers can form an ion-conducting pathway in the membrane (Bocharov *et al*., 2007). In line with these studies, BNip3 translocation into the mitochondrial membrane and BNip3 dimerization may elicit the $\Delta\psi_m$ loss observed in animal and cell culture models of HD and in myoblasts extracted from HD patients. We observed increased levels of BNip3 homodimers in the mitochondrial fractions of all HD models investigated in our studies, including human HD myoblasts, R6/2 and YAC 128 mouse brains and transfected cell lines. These data suggest that BNip3 dimerization may be a crucial step in the BNip3 activation process induced by mhtt expression, even if a role for the monomeric form of BNip3 in mitochondrial damage cannot be ruled out. Moreover, an increased resistance of the BNip3 monomeric form to PK digestion was observed in lysates from R6/2 brains and HD myoblasts. Whether some of these monomers were derived from partial dissociation of the homodimers under denaturing and reducing conditions or rather represented the molecular precursors of dimers cannot be assessed. If our hypothesis positing that BNip3 has a role in $\Delta\psi_m$ loss in HD is correct, then the inhibition of BNip3 expression and/or BNip3 translocation and dimerization in HD cells should result in the increase in mitochondrial $\Delta\psi_m$. BNip3ΔTM is a dominant-negative mutant lacking the transmembrane domain required for BNip3 translocation and integration into the OMM (Kubasiak *et al*., 2002; Regula *et al*., 2002). We observed that expression of BNip3ΔTM and simultaneous downregulation of endogenous BNip3 by RNA interference in human HD muscle cells rescued the $\Delta\psi_m$ loss induced by mutant htt. Moreover the expression of BNip3ΔTM was able to improve $\Delta\psi_m$ also in a cell line derived from the striatum of HD knock-in mice (STHdh) that represents an useful tools for examining the molecular mechanisms of HD pathogenesis.

The role of mitochondria in HD pathogenesis has long been investigated, but is poorly understood how mhtt can modulate mitochondrial network. Growing evidence indicates that the expression of mhtt results in changes to mitochondrial shape, with increased fragmentation and abnormal cristae arrangement. To investigate the effect of mhtt on mitochondrial dynamics in HD cells we examined changes in mitochondrial morphology.

In this study we demonstrate that mhtt causes abnormal mitochondrial morphology in myoblasts from HD patients and HD striatal cell lines. We next verified if we could restore normal mitochondrial morphology by expressing BNip3ΔTM in HD cells. In sum, these data demonstrate that mitochondrial morphology can be corrected in both the myoblasts from HD patients and the striatal cell model of HD by the efficient expression of a dominant-negative form of BNip3 that blocks BNip3 mitochondrial translocation.

In conclusion, our results highlighted that BNip3ΔTM expression for three days led to a significant change in mitochondrial morphologya slight (but significant) increased in JC–1 ratio and no changes in mitochondrial mass content , ATP synthesis and oxygen consumption in STHdhQ111/111 cells. No significant changes were observed in wild type STHdhQ7/7 cells. We believe, that the beneficial effects we observed in STHdhQ111/111 depend on the ability of

BNip3ΔTM to block the OMM permeabilization induced by BNip3. The low JC1 red/green that we detected in STHdhQ111/111 cells compared to STHdhQ7/7 cells likely depend on both mitochondrial depolarization and low mitochondrial content. But, the increase of the JC−1 ratio induced by BNip3ΔTM (Fig. 12c) likely reflects a real $\Delta\psi_m$ increase, since the mitochondrial mass content did not change both in STHdhQ7/7 cells and STHdhQ111/111 cells after three days of BNip3ΔTM expression.

These data support a role for BNip3 in htt-induced mitochondrial damage and point to a new potential gene therapy approach for HD. In the future, further investigations will be necessary to address BNip3 as potential target for neuroprotective therapy redirecting mhhtt cells towards survival. It is important to note that BNip3 knock-out mice are viable and lack a pathological phenotype (Diwan *et al.*, 2007); thus, the inhibition of BNip3 function by RNA interference or by overexpression of the dominant-negative mutant BNip3ΔTM may have neuroprotective effects without causing adverse side effects.

One question that remains unanswered is how mhtt induces BNip3 activation. Previous reports have shown that BNip3 association with mitochondria is strongly stabilized by acidosis or by an increased cytosolic calcium concentration. Both conditions may occur in HD cells, causing BNip3 stabilization and integration into the OMM, but one more intriguing possibility should also be considered: in light of the fact that htt can localize to the mitochondria by loosely associating with the OMM, we may hypothesize that htt binds directly or indirectly to BNip3. Future studies will aim at elucidating these and other potential mechanisms underlying the effects of mutant htt on BNip3.

Moreoverer the effect of BNip3ΔTM on mitochondrial morphology in HD cells has to be verified by ultrastructural analysis (electron microscopy), but will be necessary a viral vector encoding BNip3ΔTM to infect HD cells. A viral infection will help to demonstrate whether a stable expression of BNip3ΔTM can correct mitochondrial function such as ATP production and oxygen consumption.

References

Agnello M, Morici G and Rinaldi AM. A method for measuring mitochondrial mass and activity. Cytotechnology. 2008; 56:145-149.

Almeida S, Sarmento-Ribeiro AB, Januário C, Rego AC and Oliveira. Evidence of apoptosis and mitochondrial abnormalities in peripheral blood cells of Huntington's disease patients. Biochem Biophys Res Commun 2008; 374: 599-603.

Arenas J, Campos Y, Ribacoba R, Martin MA, Rubio JC and Ablanedo P. Complex I defect in muscle from patients with Huntington's disease. Ann Neurol 1998; 43: 397-400.

Bae BI, Xu H, Igarashi S, Fujimuro M, Agrawal N, Taya, Hayward SD, Moran TH, Montell C, Ross CA, Snyder SH and Sawa A.I. p53 mediates cellular dysfunction and behavioral abnormalities in Huntington's disease. Neuron 2005; 47: 29-41.

Bamford KA, Caine ED, Kido DK, Plassche WM and Shoulson I. Clinical-pathologic correlation in Huntington's disease: a neuropsychological and computed tomography study. Neurology. 1989; 39: 796-801.

Benchoua A, Trioulier Y, Zala D, Gaillard MC, Lefort N, Dufour, Saudou F, Elalouf JM, Hirsch E, Hantraye P, Déglon N, Brouillet E. Involvement of Mitochondrial Complex II Defects in Neuronal Death Produced by N-Terminus Fragment of Mutated Huntingtin. Mol Biol Cell 2006; 17: 1652-1663.

Benard G and Rossignol R. 2008. Ultrastructure of the mitochondrion and its bearing on function and bioenergetics. Antioxid Redox Signal. 10:1313-1342.

Bocharov EV, Pustovalova YE, Pavlov KV, Volynsk PE, Goncharuk MV and Ermolyuk YS. Unique dimeric structure of BNip3 transmembrane domain suggests membrane permeabilization as a cell death trigger. J Biol Chem 2007; 282: 16256-16266.

Bossy-Wetzel E, Petrilli A and Knott AB. Mutant huntingtin and mitochondria dysfunction. Trends Neurosci 2008; 1147: 358-382.

Browne SE. Mitochondria and Huntington's disease pathogenesis: insight from genetic and chemical models. Ann N Y Acad Sci 2008; 1147: 358-382.

Burton TR, Henson ES, Baijal P, Eisenstat DD and Gibson. The pro-cell death Bcl-2 family member, BNIP3, is localized to the nucleus of human glial cells: Implications for glioblastoma multiforme tumor cell survival under hypoxia. Int J Cancer 2006; 118: 1660-1669.

Butterworth J, Yates CM and Reynolds GP. Distribution of phosphate-activated glutaminase, succinic dehydrogenase, pyruvate dehydrogenase and gamma-glutamyl transpeptidase in post-mortem brain from Huntington's disease and agonal cases. J Neurol Sci. 1985; 67: 161-171.

Chen H, Chomyn A and Chan DC. Disruption of fusion results in mitochondrial heterogeneity and dysfunction. J Biol Chem 2005; 280: 26185-26192.

Chen G, Ray R, Dubik D, Shi L, Cizeau J and Bleackley .The E1B 19K/Bcl-2-binding protein Nip3 is a dimeric mitochondrial protein that activates apoptosis. J Exp Med 1997; 186: 1975-1983.

Ciammola A, Sassone J, Alberti L, Meola G, Mancinelli E, Russo MA, Squitieri F, Silani V. Increased apoptosis, Huntingtin inclusions and altered differentiation in muscle cell cultures from Huntington's disease subjects. Cell Death Differ. 2006; 13: 2068-2078.

Ciammola A, Sassone J, Sciacco M, Mencacci NE, Ripolone M, Bizzi C, Colciago C, Moggio M, Parati G, Silani V and Malfatto G. Low anaerobic threshold and increased skeletal muscle lactate production in subjects with Huntington's disease. Mov Disord. 2010; doi: 10.1002/mds.23258.

Costa V, Giacomello M, Hudec R, Lopreiato R, Ermak G, Lim D, Malorni W, Davies KJ, Carafoli E, Scorrano L. Mitochondrial fission and cristae disruption increase the response of cell models of Huntington's disease to apoptotic stimuli. EMBO Mol Med. 2010; 2: 490-503.

Diwan A, Krenz M, Syed FM, Wanaapura J, Ren X and Koesters AG. Inhibition of ischemic cardiomyocyte apoptosis through targeted ablation of Bnip3restrains postinfarction remodeling in mice. J Clin Invest 2007; 117: 2825-2833.

Duyao MP, Auerbach AB, Ryan A, Persichetti F, Barnes GT, McNeil SM, Ge P, Vonsattel JP, Gusella JF, Joyner AL and MacDonald, ME. Inactivation of the mouse Huntington's disease gene homolog Hdh. Science. 1995; 269: 407-410.

Frazier DP, Wilson A, Graham RM, Thompson JW, Bishopric NH and Webster. Acidosis regulates the stability, hydrophobicity, and activity of the BH3-only protein Bnip3. Antioxid Redox Signal 2006; 8: 1625-1634.

Gao S, Fu W, Dürrenberger M, De Geyter C and Zhang. Membrane translocation and oligomerization of hBok are triggered in response to apoptotic stimuli and Bnip3. Cell Mol Life Sci 2005; 62: 1015-1024.

Gárdián G and Vécsei L. Huntington's disease: pathomechanism and therapeutic perspectives. J Neural Transm. 2004; 111: 1485-1494.

Goping IS, Gross A, Lavoie JN, Nguyen, M, Jemmerson R, Roth K and Korsmeyer. Regulated targeting of BAX to mitochondria. J Cell Biol 1998; 143: 207-215.

Graham RM, Thompson JW, Wei J, Bishopric NH and Webster. Regulation of Bnip3 death pathways by calcium, phosphorylation, and hypoxia-reoxygenation. Antioxid Redox Signal 2007; 9: 1309-1315.

Hamacher-Brady A, Brady NR, Logue SE, Sayen MR, Jinno M, Kirshenbaum Gottlieb RA and Gustafsson AB. Response to myocardial ischemia/reperfusion injury involves Bnip3 and autophagy. Cell Death Differ 2007; 14: 146-157.

Harris MH and Thompson. The role of the Bcl-2 family in the regulation of outer mitochondrial membrane permeability. Cell Death Differ 2000; 7: 1182-1191.

Ho LW, Carmichael J, Swartz J, Wyttenbach A, Rankin J, and Rubinsztein DC. The molecular biology of Huntington's disease. Psychol Med. 2001; 31: 3-14.

Hodgson JG, Agopyan N, Gutekunst CA, Leavitt BR, LePiane F and Singaraja. A YAC mouse model for Huntington's disease with full-length mutant huntingtin, cytoplasmic toxicity, and selective striatal neurodegeneration. Neuron 1999; 23: 181-192.

The Huntington's Disease Collaborative Research Group. A novel gene containing a trinucleotide repeat that is expanded and unstable on Huntington's disease chromosomes. Cell. 1993; 72 :971-983.

Jenkins BG, Koroshetz WJ, Beal MF and Rosen BR.Evidence for impairment of energy metabolism in vivo in Huntington's disease using localized 1H NMR spectroscopy. Neurology. 1993; 43: 2689-2695.

Kim JY, Cho JJ, Ha J and Park. The carboxy terminal C-tail of BNip3 is crucial in induction of mitochondrial permeability transition in isolated mitochondria. Arch Biochem Biophys 2002; 398: 147-152.

Knott AB, Perkins G, Schwarzenbacher R and Bossy-Wetzel E. 2008. Mitochondrial fragmentation in neurodegeneration. Nat Rev Neurosci. 9:505-518.

Koopman WJ, Visch HJ, Smeitink JA and Willems PH. Simultaneous quantitative measurement and automated analysis of mitochondrial morphology, mass, potential, and motility in living human skin fibroblasts. Cytometry A. 2006; 69: 1-12.

Koroshetz WJ, Jenkins BG, Rosen BR and Beal MF. Energy metabolism defects in Huntington's disease and effects of coenzyme Q10. Ann Neurol. 1997; 41: 160-165.

Kubasiak LA, Hernandez OM, Bishoric NH and Webster KA. Hypoxia and acidosis activate cardiac myocite death through the Bcl-2 family protein BNIP3. Procl Natl Acad Sci USA 2002; 99:12825-12830.

Kubli DA, Ycaza JE and Gustafsson AB. Bnip3 mediates mitochondrial dysfunction and cell death through Bax and Bak. Biochem J 2007; 405: 407-415.

Landes T, Emorine LJ, Courilleau D, Rojo M, Belenguer P, Arnaune-Pelloquin L. The BH3-only Bnip3 binds to the dynamin Opa1 to promote mitochondrial fragmentation and apoptosis by distinct mechanisms. EMBO Rep. 2010; 11: 459-465.

Lee H and Paik. Regulation of BNIP3 in normal and cancer cells. Mol Cells 2006; 21: 1-6.

Legros F, Lombes A, Frachon P and Rojo M.. Mitochondrial fusion in human cells is efficient, requires the inner membrane potential, and is mediated by mitofusins. Mol Biol Cell. 2002; 13: 4343-4354.

Lodi R, Schapira AH, Manners D, Styles P, Wood NW and Taylor DJ. Abnormal in vivo skeletal muscle energy metabolism in Huntington’s disease and dentatorubropallidoluysian atropy. Ann Neurol 2000; 48: 72-76.

Mangiarini L, Sathasivam K, Seller M, Cozens B, Harper A, Hetherington C, Lawton M, Trottier Y, Lehrach H, Davies SW, Bates GP. Exon 1 of the HD gene with an expanded CAG repeat is

sufficient to cause a progressive neurological phenotype in transgenic mice. Cell 1996; 87: 493-506.

Mellor HR and Harris. The role of the hypoxia-inducible BH3-only proteins BNIP3 and BNIP3L in cancer. Cancer Metastasis Rev 2007; 26: 553-566.

Milakovic T and Johnson GV. Mitochondrial respiration and ATP production are significantly impaired in striatal cells expressing mutant huntingtin. J Biol Chem. 2005; 280: 30773-30782.

Palmfeldt J,Vang S,Stenbroen V,Pedersen CB,Christensen JH,Bross P and Gregersen N. Mitochondrial proteomics on human fibroblasts for identification of metabolic imbalance and cellular stress. Proteome Sci. 2009; 7: 20.

Panov AV, Gutekunst CA, Leavitt BR, Hayden MR, Burke JR, Strittmatter WJ and Greenamyre JT. Early mitochondrial calcium defects in Huntington's disease are a direct effect of polyglutamines.Nat Neurosci. 2002; 5: 731-736.

Panov AV, Burke JR, Strittmatter WJ and Greenamyre JT. In vitro effects of polyglutamine tracts on Ca2+-dependent depolarization of rat and human mitochondria: relevance to Huntington's disease. Arch Biochem Biophys. 2003; 410: 1-6.

Ray R, Chen G, Vande Velde C, Cizeau J, Park JH and Reed. BNIP3 heterodimerizes with Bcl-2/Bcl-X(L) and induces cell death independent of a Bcl-2 homology 3 (BH3) domain at both mitochondrial and nonmitochondrial sites. J Biol Chem 2000; 275: 1439-1448.

Regula KM, Ens K and Kirshenbaum. Inducible expression of BNIP3 provokes mitochondrial defects and hypoxia-mediated cell death of ventricular myocytes. Circ Res 2002; 91: 226-231.

Robinson BH, Petrova-Benedict R, Buncic JR and Wallace DC. Nonviability of cells with oxidative defects in galactose medium: a screening test for affected patient fibroblasts. Biochem Med Metab Biol. 1992; 48:122-126.

Saft C, Zange J, Andrich J, Muller K, Lindenberg K and Landwehmeyer B. Mitochondrial impairment in patients and asymptomatic mutation carriers of Huntington’s disease. Mov Dis 2005; 20: 674-679.

Sassone J, Colciago C, Cislaghi G, Silani V and Ciammola A. Huntington's disease: the current state of research with peripheral tissues. Exp Neurol. 2009; 219: 385-397.

Sawa A, Wiegand GW, Cooper J, Margolis RL, Sharp AH, Lawler JF Jr, Greenamyre JT, Snyder SH and Ross CA. Increased apoptosis of Huntington disease lymphoblasts associated with repeat length-dependent mitochondrial depolarization. Nat Med 1999; 5: 1194-1198

Squitieri F, Falleni A, Cannella M, Orobello S, Fulceri F, Lenzi P and Fornai F. Abnormal morphology of peripheral cell tissues from patients with Huntington disease. J Neural Transm. 2010; 117: 77-83.

Stahl WL and Swanson PD. Biochemical abnormalities in Huntington's chorea brains. Neurology. 1974; 24: 813-819.

Tracy K and Macleod. Regulation of mitochondrial integrity, autophagy and cell survival by BNIP3. Autophagy 2007; 3: 616-619.

Trettel F, Rigamonti D, Hilditch-Maguire P, Wheeler VC, Sharp AH, Persichetti F, Cattaneo E and MacDonald ME. 2000. Dominant phenotypes produced by the HD mutation in STHdh(Q111) striatal cells. Hum Mol Genet. 9:2799-2809.

Vande Velde C, Cizeau J, Dubik D, Alimonti J, Brown T and Israels. BNIP3 and genetic control of necrosis-like cell death through the mitochondrial permeability transition pore. Mol Cell Biol 2000; 20: 5454-5468.

Vonsattel JP, DiFiglia M. Huntington disease. J Neuropathol Exp Neurol. 1998; 57: 369-84.
Wang H, Lim PJ, Karbowski M and Monteiro MJ. 2009. Effects of overexpression of huntingtin proteins on mitochondrial integrity. Hum Mol Genet. 18:737-752.

Webster KA, Graham RM and Bishopric. BNip3 and signal-specific programmed death in the heart. J Mol Cell Cardiol 2005; 38: 35-45.